Investigating EV as a mechanism mediating the cellular effects of adiponectin

Wing Yan (Trista) Chung

A thesis submitted to the Faculty of Graduate Studies in partial fulfillment of the requirements for the degree of Master of Science

Graduate Program in Biology
York University, Toronto, Ontario
August 2025

Abstract

Adiponectin provides systemic protection in cardiometabolic health, yet the mechanisms underlying its tissue-specific effects remain poorly understood due to its functional complexity. Therapeutic development is further hindered by difficulties in generating stable, bioactive forms with sustained and targeted activity. Emerging evidence highlights extracellular vesicles (EV) as mediators of inter-organ communication and promising vehicles for the development of new therapeutics. This thesis investigates the cardioprotective role of plasma or adipocyte-derived EV isolated from mice that were treated with or without the adiponectin-mimetic peptide ALY688. EV isolated from adipocytes after mice were treated with ALY688, versus control, enhanced autophagic flux plus reduced reactive oxygen species, caspase-3/7 activation, and cell death in H9c2 cardiomyoblasts under hypoxia ± reoxygenation. EV were also isolated from HEK cells genetically modified to overexpress adiponectin and compared to wild-type cells. These EV improved insulin sensitivity in L6 skeletal muscle cells. This study identifies a previously uncharacterized role of adiponectin in modulating EV biogenesis and cargo to elicit cardioprotective and beneficial metabolic effects. This demonstrates the potential of EV-based adiponectin therapeutics as a new strategy for treating cardiometabolic diseases.

Acknowledgements

I am sincerely grateful to Dr. Gary Sweeney for the opportunity to pursue my Master's degree under his mentorship. I also extend my appreciation to the members of the Sweeney lab for their continuous support, with special thanks to Dr. Hyekyoung (Cindy) Sung for her valuable guidance throughout the project. I would like to thank Dr. Terrance Kubiseski for his thoughtful feedback on my research and for chairing my thesis defence. I am also thankful to my examining committee members, Dr. Ali Abdul-Sater and Dr. Steven Connor, for generously dedicating their time to review and evaluate my thesis. Lastly, I am grateful for the opportunity to conduct research in Dr. Ssang-Goo Cho's lab, supported by the Mitacs Globalink Research Award.

Abbreviations

AMPK – AMP-activated protein kinase
ATP – Adenosine triphosphate
BSA – Bovine serum albumin
CMD – Cardiometabolic disease
COX-2 – Cyclooxygenase-2
CVD – Cardiovascular disorders
DMEM – Dulbecco's Modified Eagle Medium
EV – Extracellular vesicles
FBS – Fetal bovine serum
GFP – Green fluorescent protein
HEK – Human embryonic kidney
HFD – High-fat diet
HIF – Hypoxia-inducible factor
HMW – High molecular weight
H/R – Hypoxia/reoxygenation
IRI – Ischemia/reperfusion injury
ISEV – International Society for Extracellular Vesicles
MASH – Metabolic dysfunction-associated steatohepatitis
MSCs – Mesenchymal stem cells
NTA – Nanoparticle tracking analysis
PBS – Phosphate-buffered saline
PenStrep – Penicillin-streptomycin
PPAR – Peroxisome proliferator-activated receptor
ROS – Reactive oxygen species
SEC – Size exclusion chromatography
TZD – Thiazolidinedione
WB – Western blot
WJMSCs – Wharton's jelly-derived mesenchymal stem cells
WT – Wild type

Table of Contents

1 Chapter 1: Literature Review

1.1 Physiology of Adiponectin

Adiponectin is an adipocyte-derived hormone critically involved in regulating systemic metabolic homeostasis. It is primarily secreted by mature adipocytes within white adipose tissue (WAT), the body's largest endocrine organ [1]. Although adipocytes are the predominant source, lower expression levels of adiponectin are also detected in cardiomyocytes [2, 3], skeletal muscle cells[3], and quiescent hepatic stellate cells [4]. Under basal physiological conditions, adiponectin is constitutively secreted into circulation, maintaining relatively stable plasma concentrations [5]. However, plasma adiponectin levels increase during energy-deficient states such as fasting[6], caloric restriction, and physical exercise [7]. Additionally, factors including activation of peroxisome proliferator-activated receptor gamma (PPARγ), adipocyte differentiation [8], adipocyte size, and endoplasmic reticulum (ER) stress significantly influence adiponectin secretion rate and oligomeric form [9].

Structurally, adiponectin is synthesized as a 244-amino-acid protein [7] undergoing essential post-translational modifications that yield bioactive conformations [10]. In circulation, adiponectin exists in distinct oligomeric forms: trimers, hexamers and high-molecular-weight (HMW) (12- 18mers) multimers [10]. Among these, HMW adiponectin is the most potent in enhancing insulin sensitivity [5], particularly in insulin-responsive tissues such as skeletal muscle and liver [11]. In addition to full-length adiponectin, an innate immune protein c1q-like globular form generated through proteolytic cleavage exhibits strong biological activity in muscle, promoting fatty acid oxidation [12] and muscle

differentiation [13]. This diversity allows adiponectin to engage multiple receptor types, mediating a wide range of metabolic and cellular functions across tissues.

The human adiponectin gene (ADIPOQ) resides within a genetic locus associated with susceptibility to type 2 diabetes and metabolic syndrome [14, 15], suggesting adiponectin as the potential causative gene. Beyond metabolic regulation, adiponectin also exerts beneficial effects on various organs, including the brain, heart, kidneys, and bone [7], intestines [16], pancreas, endothelium [17], and immune systems [18].

1.2 Adiponectin in Cardiometabolic Health

Adiponectin is a critical regulator of cardiometabolic health, displaying protective roles against metabolic and inflammatory disorders, including type 2 diabetes, metabolic dysfunction-associated steatohepatitis (MASH; formerly known as non-alcoholic fatty liver disease), obesity [19], and cardiovascular disorders (CVD) [20]. Clinically, high circulating adiponectin levels correlate with healthy metabolism, whereas low adiponectin levels (hypoadiponectinemia) are common in obesity, insulin resistance, and chronic inflammatory conditions [21].

Adiponectin exerts metabolic regulation primarily through two transmembrane receptors: AdipoR1, abundant in skeletal muscle and endothelial cells, and AdipoR2, predominant in the liver [22]. Binding of adiponectin to these receptors activates downstream signaling pathways such as AMP-activated protein kinase (AMPK) and PPARα [22, 23]. Activation of these pathways enhances glucose uptake [24], lipid oxidation [23, 24], mitochondrial

function [25], insulin sensitivity[22], and prevents lipotoxicity [23, 24]. Additionally, adiponectin suppresses hepatic gluconeogenesis, contributing to enhanced glucose homeostasis [26, 27].

In addition to its transmembrane receptors, adiponectin also binds T-cadherin, a glycosylphosphatidylinositol (GPI)-anchored receptor selectively expressed in eukaryotic cells that specifically bind to HMW adiponectin [28]. T-cadherin is highly expressed in the myocardium, where it facilitates localized adiponectin signaling and is essential for mediating its cardioprotective effects via AMPK activation [29].

Mechanistically, adiponectin confers cardioprotection by reducing oxidative and nitrative stress, mitigating inflammation, and enhancing fatty acid oxidation through the activation of essential signaling pathways such as AMPK and cyclooxygenase-2 (COX-2) [30-33]. These combined effects significantly contribute to the attenuation of pathological cardiac remodeling and ischemic damage [34].

Adiponectin also promotes autophagy, an essential process in maintaining cellular energy balance and organelle integrity, mediated primarily via AMPK activation and inhibition of the mammalian target of rapamycin (mTOR) pathway [35]. Autophagy regulation by adiponectin is particularly vital in metabolically active tissues such as the liver, heart, and skeletal muscle, supporting mitochondrial turnover, lipid clearance, and protection from oxidative stress [36].

Furthermore, adiponectin significantly impacts cellular sphingolipid metabolism by exerting intrinsic ceramidase activity through its receptors. Ceramide is a class of sphingolipid, and increased levels are linked to insulin resistance, cardiovascular diseases and type 2 diabetes [37]. This activity reduces intracellular ceramide concentrations, thereby enhancing insulin sensitivity and promoting cell survival [38]. Together, these signaling and metabolic functions underscore adiponectin's role as a central regulator of systemic energy balance, cellular stress responses, and metabolic homeostasis under pathophysiological conditions. Uniquely among hormones, adiponectin exerts broad protective effects across multiple organ systems while modulating a wide range of critical cellular pathways.

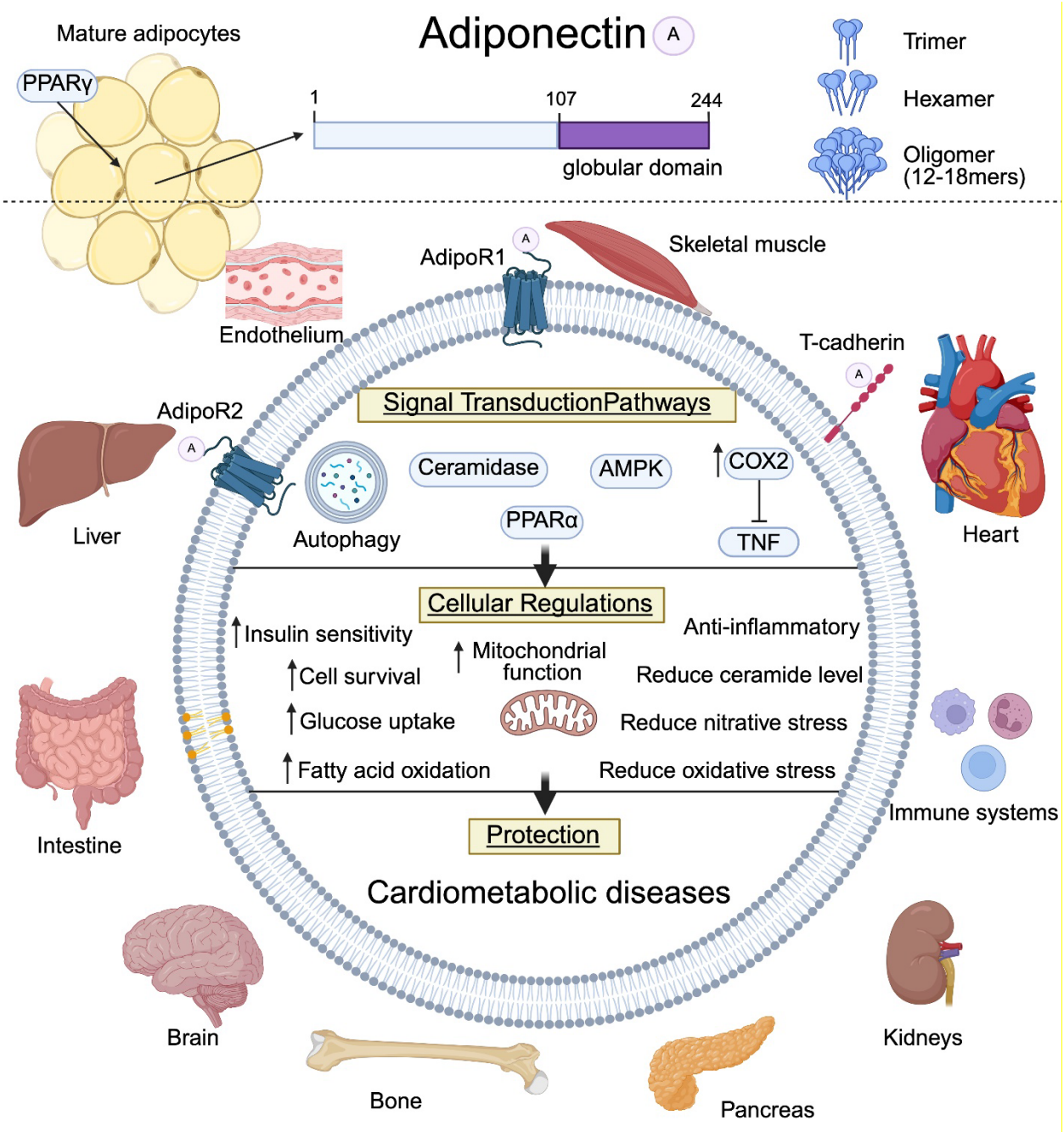

Figure 1: Overview of adiponectin and signaling pathways (Summary of sections 1.1 and 1.2). Adiponectin is produced by mature adipocytes and binds to AdipoR1 (primarily in skeletal muscle) and AdipoR2 (primarily in liver), activating downstream pathways including AMPK, PPARα/γ, COX-2, and autophagy. These signaling cascades regulate cellular processes such as glucose uptake, fatty acid oxidation, mitochondrial function, and inflammation, ultimately contributing to protection against type 2 diabetes (T2D), metabolic dysfunction-associated steatohepatitis (MASH), cardiovascular disorders (CVD), and obesity. Surrounding organs or systems represent adiponectin-responsive cells or tissues being studied. (created using BioRender.com)

1.3 Adiponectin Therapeutics: Challenges and Prospects

Despite promising preclinical evidence of adiponectin-based therapies, several translational barriers persist. These include the protein's structural complexity, challenges in producing stable and biologically active recombinant forms, and rapid hepatic clearance that limits its therapeutic efficacy [5, 39]. To address these limitations, synthetic agonists of adiponectin receptors, such as AdipoRon and ALY688, have been developed. AdipoRon is a small-molecule agonist [40], while ALY688 is a small peptide agonist [41]. Both activate AdipoR1 and AdipoR2, thereby activating adiponectin's downstream signaling effects, including AMPK and PPAR pathways [40, 42].

These agonists have demonstrated efficacy in multiple models of cardiometabolic diseases (CMD). AdipoRon improves cardiac function in heart failure with preserved ejection fraction by reducing myocardial lipid accumulation and fibrosis through enhanced fatty acid oxidation [43]. It also enhances mitochondrial function and reduces muscle degeneration in obese mice [44]. ALY688 enhances insulin sensitivity in skeletal muscle by increasing both basal and insulin-stimulated glucose uptake [45], and exerts cardioprotective effects in pressure overload-induced heart failure by attenuating hypertrophy, fibrosis, and inflammation while improving metabolic remodeling [46].

Despite these encouraging findings, concerns about systemic exposure, long-term safety, and off-target effects remain unresolved. Targeted delivery strategies are therefore under investigation to enhance therapeutic precision and efficacy [47]. Among these, extracellular vesicles (EV) have emerged as promising carriers of therapeutic molecules,

enabling stable, tissue-specific delivery while minimizing immune clearance through their natural role in intercellular communication [48]. Their application will be discussed in the following section.

1.4 Biological Properties of Extracellular Vesicles

EV are membrane-bound nanoparticles (30–1000 nm in diameter) secreted by various cell types, mediating intercellular and interorgan communication through the transport of bioactive signaling molecules [48, 49]. EV are heterogeneous in size, biogenesis mechanisms, and cargo composition. Based on their formation pathways, EV are often classified as exosomes and ectosomes [48]. Exosomes originate from the inward budding of endosomal membranes, followed by their release through exocytosis [50]. In contrast, ectosomes, which include microvesicles and apoptotic bodies (up to 4000 nm), form directly by outward budding from the plasma membrane [50]. Due to challenges in isolating and characterizing pure EV subtypes, current guidelines by International Society for Extracellular Vesicles (ISEV) advocate a simplified classification into large EV and small EV (< 200 nm) [51]. Studies commonly separate EV populations by size, as they have different cargo and biological effects [52].

The biological relevance of EV arises from their selectively packaged cargo, which includes DNA, mRNA, lncRNA, miRNA, proteins, lipids [53] and even mitochondria [54]. This cargo composition is not randomly assembled but reflects the type and physiological state of the parent cells, thereby determining the biological effects of EV on recipient cells

[55]. Consequently, EV function as critical mediators of intercellular communication, transmitting functional status and pathophysiological signals from their cells of origin [56].

1.5 Therapeutic Potential of Extracellular Vesicles

EV have unique features, such as natural cargo delivery, membrane stability that ensures cargo protection, capabilities for targeted and systemic signaling, low immunogenicity (triggering minimal host immune responses), acellular nature, and capacity to deliver complex biomolecules, making them highly promising for therapeutic interventions [57]. EV can also serve as valuable biomarkers for various disease conditions, as their cell-specific cargo reflects pathophysiological changes and the tissue or organ of origin [56], offering information that traditional blood-based biomarkers often fail to provide [53]. Moreover, EV can be isolated from a variety of biological fluids beyond blood, including cerebrospinal fluid, lymph fluid, urine [53], saliva, semen [58], and breast milk [59], expanding their utility for non-invasive biomarker discovery across diverse clinical settings.

Recent clinical progress has highlighted the therapeutic and diagnostic potential of EV, with multiple phase III trials underway for conditions including COVID–19–associated acute respiratory distress syndrome, retinitis pigmentosa, and ear infections [57]. Additionally, the U.S. Food and Drug Administration has granted Breakthrough Device Designation to an EV–based urine test for prostate cancer, recognizing its superior non-invasive performance over traditional risk assessment tools [57]. In cardiovascular diseases, EV have attracted significant attention not only as diagnostic biomarkers but

also as critical signaling entities and promising therapeutic agents. Their anti-inflammatory properties and ability to promote cardiac tissue repair and regeneration following MI demonstrated their therapeutic potential [60].

A wide range of existing and emerging EV delivery methods have been developed, including topical application, injection, oral and nasal administration, and incorporation into hydrogels or microneedles [61]. Alongside these delivery strategies, bioengineering approaches further enhance the therapeutic potential of EV by enabling more tailored and effective applications. These strategies include optimizing EV potency, cargo loading, targeted or localized delivery, circulation half-life, cellular uptake efficiency, and resistance to lysosomal degradation [57].

To enhance EV potency, the incorporation of vesicular stomatitis virus glycoprotein (VSV-G) has been shown to improve endosomal escape and increase the bioactivity of EV-delivered proteins [62]. Efficient cargo loading can be achieved through passive incubation with therapeutic agents or through active methods such as electroporation, sonication, freeze-thaw cycles, and transfection, which facilitate the incorporation of diverse therapeutic materials into EV [63].

For targeted delivery, EV engineered with ischemic myocardium-homing peptides significantly improve myocardial retention and localized therapeutic effects in myocardial infarction models [64, 65]. Systemic circulation time can be extended by enriching EV

membranes with CD47, a “don’t eat me” signal that reduces mononuclear phagocyte system-mediated clearance [66].

To further enhance therapeutic retention and localized action, incorporating MSCs EV into injectable hydrogels, such as sodium alginate, has been shown to sustain EV release within infarcted myocardium and promote cardiac repair following MI [67]. This hydrogel-based approach not only protects EV from rapid clearance but also provides a physical scaffold for gradual therapeutic delivery.

Cellular uptake can also be optimized by functionalizing EV with arginine-rich cell-penetrating peptides, which enhance entry via macropinocytosis and facilitate cytosolic delivery [68]. Additionally, to prevent lysosomal degradation and promote efficient intracellular release, pH-sensitive fusogenic peptides like GALA can be incorporated into EV membranes, facilitating endosomal escape and cytosolic delivery of functional cargo [69].

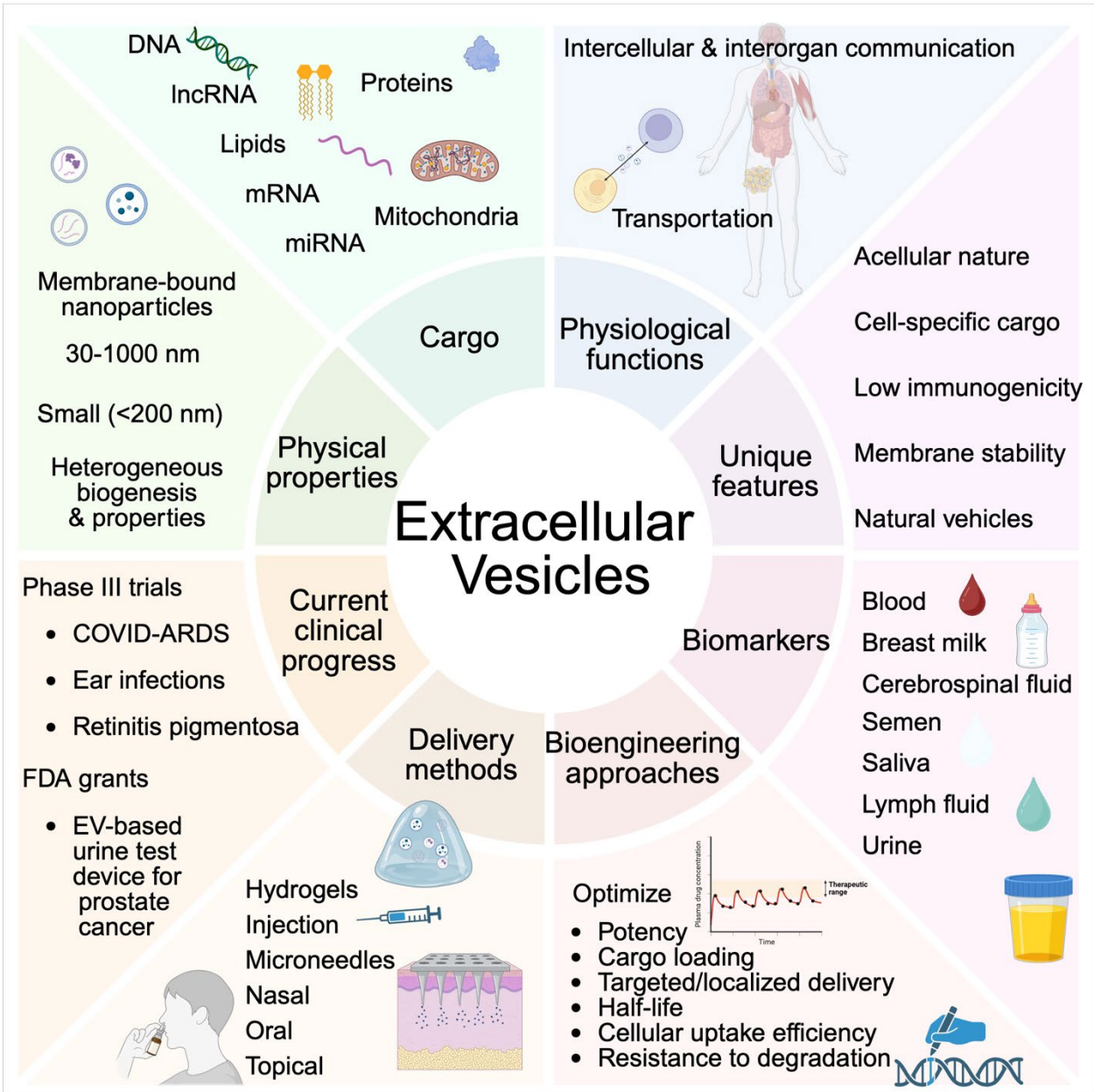

Figure 2: Overview of extracellular vesicles (EV): biogenesis, composition, and therapeutic applications. (Summary of sections 1.4 and 1.5) EV are membrane-bound nanoparticles ranging from 30 to 1000 nm in diameter, classified into small (<200 nm) and large populations with heterogeneous biogenesis. They carry diverse bioactive cargos and mediate intercellular and interorgan communication. Unique features of EV contribute to their potential for therapeutic intervention and use as biomarkers. EV can be isolated from a wide range of sources for biomarker detection. They can also be engineered for advanced therapeutic effects with various modes of administration. Current clinical progress sheds light on the development of EV-based therapies. (created using BioRender.com)

1.6 Extracellular Vesicles and Adiponectin

Recent studies have demonstrated that adiponectin regulates the production of small EV, contributing to systemic metabolic homeostasis and exerting cardioprotective effects [70, 71]. In mesenchymal stem cells (MSCs), adiponectin promotes EV release, enhancing their therapeutic efficacy in heart failure models through mechanisms essential for intercellular signaling and tissue repair [72]. The functional link between adiponectin signaling and EV biogenesis underscores the relevance of EV as effectors of adiponectin-mediated benefits in cardiometabolic disorders.

EV carrying adiponectin have been shown to possess anti-inflammatory and insulin-sensitizing properties, which may underlie their protective effects in the heart [73-75]. Adipocyte-derived EV (Ad-EV), a major subset of circulating EV, are efficiently taken up by cardiac tissue and modulate cardiac function through their bioactive cargo [76]. These vesicles contain adipokines, cytokines, enzymes, and regulatory microRNAs [54, 75, 77-80]. Through these components, Ad-EV influence lipid metabolism, reduce inflammation, and improve insulin sensitivity, processes that are central to myocardial recovery following myocardial infarction (MI) and ischemia/reperfusion injury (IRI) [81, 82].

Adiponectin has also been reported to associate with the EV surface via adsorption, independent of the EV cellular origin [83]. Ad-EV isolated from lean mice, enriched with surface-bound adiponectin, reduced inflammation, enhanced insulin sensitivity, and attenuated weight gain in HFD models [83]. These findings highlight the role of adiponectin and Ad-EV in concert to regulate systemic metabolism and protect against

cardiac injury. Investigating adiponectin-EV interactions may therefore provide novel insights and solutions to current therapeutic obstacles.

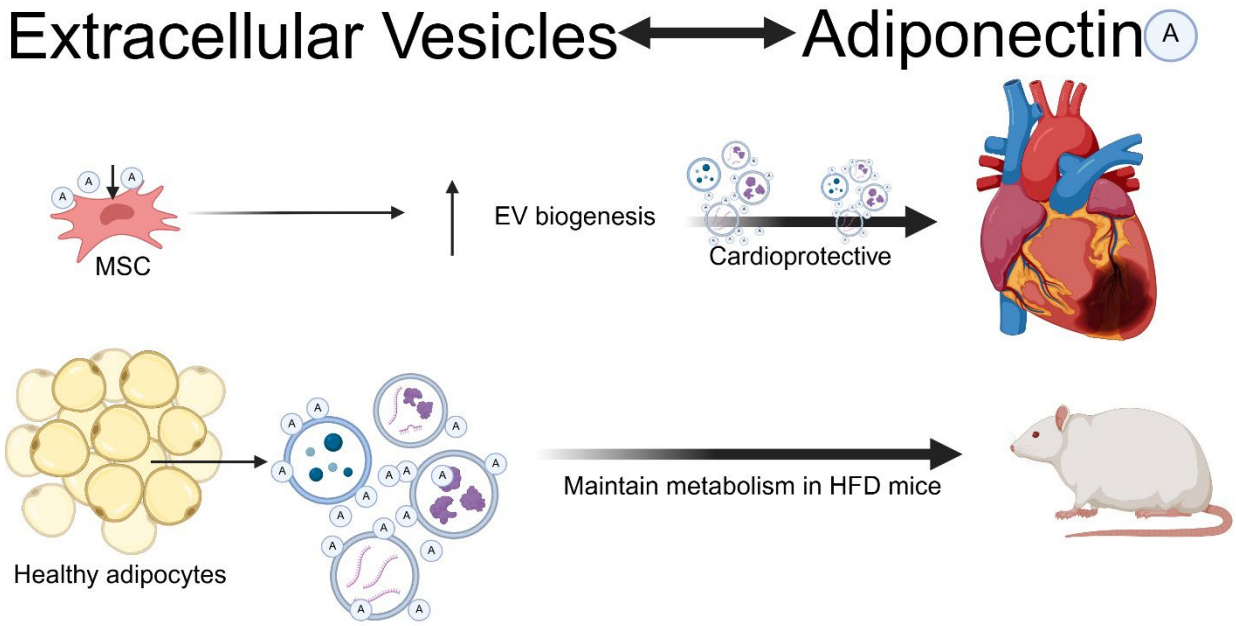

Figure 3: Adiponectin regulates extracellular vesicle (EV) biogenesis and function in cardiometabolic health. (Summary of section 1.5) Adiponectin enhances EV biogenesis in mesenchymal stem cells (MSC) and exert cardioprotective effects. Adipocyte-derived EV (Ad-EV), enriched with adiponectin on the surface by adhesion and bioactive molecules such as adipokines and miRNAs have been shown to maintain metabolic homeostasis in high-fat diet (HFD) models, highlighting the therapeutic relevance of adiponectin-EV interplay in cardiometabolic health. (created using BioRender.com)

1.7 Research Aims and Hypothesis

Adiponectin is an adipokine known for its beneficial effects on insulin sensitivity, oxidative stress reduction, and cardioprotection. Although its systemic actions are well established, the underlying mechanisms that mediate tissue-specific effects, particularly those involving EV-mediated crosstalk, remain underexplored. Moreover, the clinical application of adiponectin has been hindered by its instability, short half-life, and challenges in producing bioactive multimeric forms. The objectives of this thesis are to investigate the potential role of EV in mediating adiponectin-associated cardioprotection (Study 1) and to examine whether EV can serve as effective carriers for functional adiponectin delivery (Study 2). Investigating the functional role of EV in adiponectin-based therapies may allow novel pathways and mechanisms, thereby advancing our understanding and guiding the development of novel therapeutic strategies to mitigate disease progression and mortality in metabolic and cardiovascular disorders.

Study 1: The role of ALY-Ad-EV in cardioprotection under hypoxia and hypoxia/reoxygenation in H9c2 cells

In our previous studies, vesicles were observed in cardiac tissue by scanning electron microscopy (SEM) from ALY688-treated IRI rats, suggesting a potential involvement of EV in the protective effects. Given that adiponectin is secreted by and exhibits a positive autocrine effect on adipocytes [84], and that Ad-EV carry adiponectin in circulation, ALY688 may influence Ad-EV cargo composition. This study investigates the potential role of EV in mediating adiponectin-associated effects in response to ALY688 treatment, with a focus on cardiomyocyte protection. Using an in vitro model, I examined the effects

of ALY-Ad-EV on H9c2 cardiomyoblasts subjected to hypoxia (H) and hypoxia/reoxygenation (H/R) to simulate MI and IRI, respectively. Oxidative stress, autophagy, caspase-3/7 activation, and cell viability were examined. I hypothesize that ALY-Ad-EV will protect against H and H/R injury in H9c2 cells, potentially through mechanisms resembling adiponectin activity, such as enhancing autophagy, reducing oxidative stress, caspase 3/7 activation and cell death.

Study 2: The role of adiponectin-overexpressing EV (Ad-OE-EV) in enhancing insulin sensitivity in L6 cells

The second study investigates the therapeutic potential of engineered EV derived from adiponectin-overexpressing Wharton's jelly mesenchymal stem cells (WJMSCs) and human embryonic kidney (HEK) cells (Ad-OE-EV). These EV were applied to L6 skeletal muscle cells to evaluate their ability to enhance insulin sensitivity by modulating insulin signaling pathways. I hypothesize that Ad-OE-EV are enriched with functional adiponectin and will improve insulin sensitivity in L6 cells, supporting their potential as a cell-free therapeutic strategy for metabolic disease intervention. Accordingly, I propose that Ad-OE-EV will increase insulin-stimulated Akt activation and glucose uptake.

2 Chapter 2: Adipocyte-derived EV mediating adiponectin effects

2.1 Abstract

Myocardial ischemia/reperfusion injury (IRI) is a major cause of cardiac dysfunction following myocardial infarction (MI), primarily driven by oxidative stress and irreversible cardiomyocyte death. While adiponectin is known for its cardioprotective effects, the mechanisms underlying its systemic actions remain unclear. This study investigated whether extracellular vesicles (EV) mediate adiponectin-induced cardioprotection. EV were isolated from adipocytes (ALY-Ad-EV) and plasma (ALY-plasma-EV) of mice treated with ALY688, an adiponectin receptor agonist, and tested in H9c2 under hypoxia (H) and hypoxia/reoxygenation (H/R). Both ALY-Ad-EV and ALY-plasma-EV enhanced autophagic flux, and reduced caspase-3/7 activation and cell death under H. Under H/R, both EV types reduced oxidative stress, but only ALY-Ad-EV reduced caspase-3/7 activation and cell death. These findings suggest that adiponectin may promote cardioprotection not only through direct actions on the heart, but also by interacting with other organs, such as adipose tissue, to influence EV dynamics with protective effects.

2.2 Introduction

Ischemic heart disease (IHD), characterized by myocardial blood supply reduction due to coronary artery occlusion, remains a leading global cause of mortality [85]. While timely reperfusion therapy is critical for treating myocardial infarction (MI), it paradoxically exacerbates tissue damage through IRI, which involves oxidative stress, calcium overload, inflammation, and microvascular dysfunction [85, 86]. Although acute-phase mortality from MI has declined to historic lows due to advances in reperfusion strategies, long-term complications such as heart failure and major adverse cardiovascular events remain common, particularly in aging populations and regions with high MI prevalence [87]. These challenges highlight the ongoing need for effective therapies targeting both MI and IRI.

Adiponectin is a well-characterized cardioprotective adipokine. Studies have shown its therapeutic potential in both MI and IRI models. Adiponectin knockout mice exhibit more severe injury, whereas exogenous adiponectin reduces oxidative stress and caspase-3 activation in cardiomyocytes through calreticulin, independent of AMPK signaling [88]. Although low circulating adiponectin is associated with adverse cardiovascular outcomes, recent evidence suggests that the effectiveness of adiponectin signaling in MI and IRI depends more on receptor sensitivity than on circulating levels alone, emphasizing the importance of functional adiponectin responsiveness over its absolute concentration [89]. For instance, pathological modifications of AdipoR1 can impair its signaling capacity and contribute to cardiovascular dysfunction [90]. Also, a study identified that phosphorylation of adiponectin receptor 1 (AdipoR1) at Ser7 during ischemic stress impairs downstream

signaling. Preventing this modification restores AdipoR1 activity and improves cardiac function following IRI [91].

In addition to its well-established direct effects on target tissues, adiponectin may influence EV composition and functions, particularly from adipocytes. As the primary endocrine cell type in adipose tissue, adipocytes play a central role in systemic metabolic regulation and inter-organ communication through EV secretion. Ad-EV actively mediate signaling between adipose tissue and the heart, influencing cardiac function under both physiological and pathological conditions. Notably, the cargo and function of Ad-EV are altered in metabolic disorders such as obesity and diabetes, which can significantly impact cardiovascular outcomes [76]. For instance, Ad-EV derived from diabetic adipose tissue has been shown to worsen ischemic heart injury by promoting oxidative stress and mitochondrial apoptosis in cardiomyocytes, driven by changes in miRNA and protein cargo, such as reduced miR-130b and increased pro-apoptotic signals [92]. Conversely, Ad-EV from lean adipose tissue may carry protective signals that mitigate mitochondrial dysfunction and inflammation in cardiomyocytes, highlighting the context-dependent nature of their cardiac effects [76, 93]. These findings underscore the importance of Ad-EV as both mediators and potential therapeutic targets in CMD.

Adiponectin also acts in an autocrine fashion on adipocytes by activating PPARγ, which promotes further adiponectin production [84], downregulates cytokine secretion [94] and enhances EV production. Accordingly, it is expected that ALY688 would increase Ad-EV enriched with adiponectin, amplifying systemic and cardiac protective effects.

To study the role of ALY-Ad-EV in cardiomyocyte injury, an in vitro model was employed using H9c2 under hypoxia (H) and hypoxia/reoxygenation (H/R) conditions (Fig. 4). These models reproduce core pathophysiological features of MI and IRI, respectively, which have distinct features on cellular injury (Table 1). Although lacking systemic components such as immune infiltration or vascular remodeling, this system allows focused investigation of oxygen-related cellular pathways. In this study, H was set as 24 h of oxygen deprivation, while H/R consisted of 6 h of H followed by R periods up to 24 h. Cellular responses differ markedly between these conditions. Chronic H (24 h) in H9c2 leads to decreased cell viability along with induction of HIF-1α expression, elevates intracellular calcium, and reduces adenosine triphosphate (ATP) and ROS levels [95]. In contrast, H/R elicits a burst of oxidative stress during reoxygenation, triggering mitochondrial fission, calcium dysregulation, and caspase-mediated apoptosis [96, 97].

Table 1. Comparison of regulated cell death mechanisms and injury features between myocardial infarction (MI) and myocardial ischemia/reperfusion injury (IRI) [98].

Feature	MI	IRI
Regulated death pathways	Primarily apoptosis and necrosis	Strong activation of necroptosis, ferroptosis, and pyroptosis
Primary cause of death	ATP depletion due to prolonged oxygen/glucose loss	Oxidative stress, calcium overload, mitochondrial damage
Mitochondrial role	Mitochondrial damage accumulates slowly	Sudden massive injury during reperfusion
ROS	Low ROS	Burst of ROS upon reoxygenation damages DNA, proteins, and lipid membranes

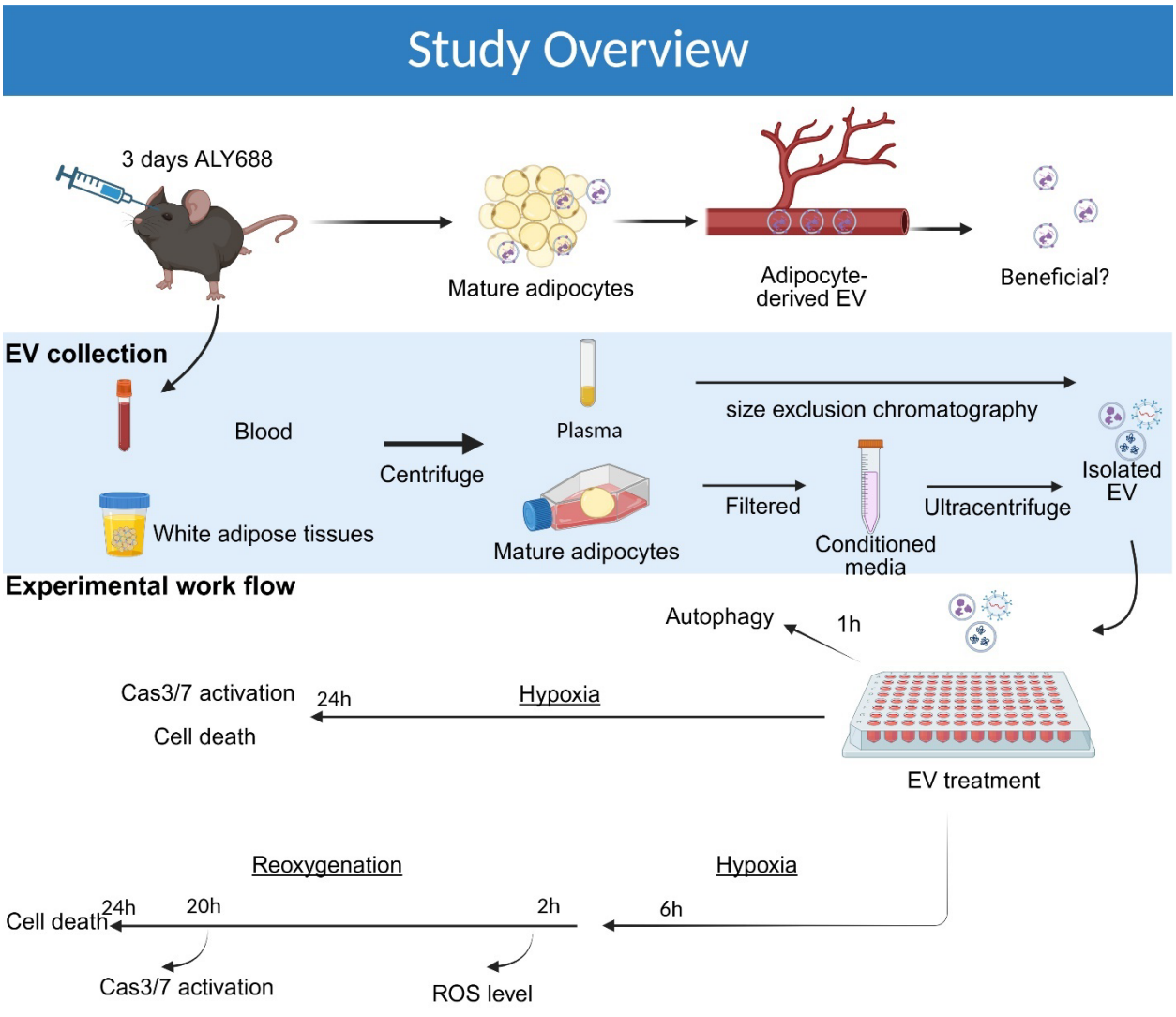

Figure 4. Schematic overview of the study design and experimental workflow.

In this study, Ad-EV and plasma-EV were isolated from mice following a 3-day injection of PBS or ALY688 and applied to an in vitro model of hypoxia (H) and hypoxia/reoxygenation (H/R) injury in H9c2. Plasma-EV were analyzed alongside Ad-EV to provide a systemic perspective, as Ad-EV are expected to reach the heart via circulation, while plasma-EV may contain vesicles released from other tissues in response to ALY688. This comparison aimed to determine whether Ad-EV are the principal mediator of adiponectin's protective effects. I hypothesized that under energy stress induced by H or H/R, ALY-induced Ad-EV would protect H9c2 cells by reducing oxidative stress, caspase 3/7 activation, and cell death.

2.3 Materials and Methods

In vitro cell cultures

Wild-type H9c2 (ATCC, CRL-1446™) rat embryonic cardiomyoblasts were used for in vitro studies. Cells were stored at -80°C or cultured in complete medium consisting of 10% fetal bovine serum (FBS) (WISENT, #080-150) and 1% penicillin-streptomycin (PenStrep) (Gibco, #15140) in 1 g/L D-glucose Dulbecco's Modified Eagle's Medium (DMEM) (Gibco, #11885). Unless otherwise specified, all cultures were maintained at 37°C with 5% carbon dioxide (CO2) and subcultured upon reaching 80% confluency.

Animal care and use

All animal procedures were approved by the York University Animal Care Committee and adhered to the Canadian Council on Animal Care guidelines. 10–13-week-old male wild-type C57BL/6 mice (Charles River, #C57BL/6) were housed in a controlled environment with a 12 h light/12 h dark cycle, stable temperature, and free access to a standard rodent chow diet (Lab Diet 5015) and water. Mice were acclimatized for at least one week before experiments and randomized to receive daily subcutaneous injections of either phosphate-buffered saline (PBS; Gibco, #10010049) or ALY688 (15mg/kg) (Allysta Pharmaceuticals) for three consecutive days.

Isolation of EV from conditioned media of primary adipocytes

Inguinal and epididymal adipose tissues were dissected from mice and minced using sterile scissors and blades. Tissues (every 1-1.2g) were washed with sterile PBS and digested in 5 mL Krebs-Ringer bicarbonate HEPES(KRBH) buffer containing 1 mg/mL type II collagenase (Sigma, #C2-22-1g) for 45 min at 37°C with shaking. The digested

tissue was filtered through a sterile 500 µm nylon mesh to remove undigested structures and centrifuged at 60 × g for 2 min to separate mature adipocytes from the stromal vascular fraction (non-adipocyte cells) and tissue debris. The buffer beneath the adipocyte layer was removed, and the adipocyte layer was washed twice with KRBH buffer. Primary adipocytes were cultured in 10 mL serum-free 1 g/L D-glucose DMEM with 1% PenStrep in T-25 culture flasks at 37°C for 20 hr. The conditioned medium was centrifuged at 300 × g for 10 min, transferred to a new tube, and centrifuged at 1200 × g for 10 min. It was then filtered using a 0.45 µm Filtropur S filter (Sarstedt, #83.1826) and stored at -80°C. EV were isolated by ultracentrifugation at 100,000 × g for 1.5 hr at 4°C, after which the supernatant was discarded and the EV pellet resuspended in PBS filtered by 0.2 µm syringe filter (Basix, #13100106).

Collection of plasma and isolation of circulating EV

Blood samples were collected in ethylenediaminetetraacetic acid (EDTA) tubes (Becton Dickinson, #367844), which chelate calcium to prevent coagulation, and incubated at room temperature for 1 hr. Tubes were centrifuged at 2000 × g for 10 min at room temperature, and the plasma from the supernatant was collected and stored at -80°C. 100 µL of plasma per sample was centrifuged through an Amicon 15 filter with a 100 kDa cutoff to purify samples from proteins or other molecules smaller than EV. Supernatant was collected and EV were isolated via size exclusion chromatography (SEC) using an automated fraction collector (Izon, AFC-V2) and qEV single 70 nm columns (Izon). WB analysis confirmed EV presence, and EV-positive fractions were pooled for further experiments.

Western blot

Samples were lysed in buffer (pH 6.8 Tris-HCl, 10% SDS, glycerol, ddH2O) supplemented with Pierce Protease and Phosphatase Inhibitor Mini Tablets (1 tablet/10 mL) (Thermo, #A32959). Lysates were centrifuged at 10,000 rpm at 4°C for 10 min. Protein concentrations were determined using the Pierce™ Bicinchoninic Acid (BCA) Protein Assay Kit (Thermo, #23225), and samples were normalized by adding loading buffer and ddH2O. Equal amounts of protein were separated by SDS-PAGE (8% - 15%) and transferred to polyvinylidene difluoride (PVDF) membranes. Membranes were blocked with 5% BSA/milk for 1 h at room temperature, followed by overnight incubation with primary antibodies at 4°C. HRP-conjugated secondary antibodies were incubated for 1 h at room temperature.

List of antibodies used: Cell signalling (Alix #92880, anti-rabbit IgG #7074), Invitrogen (CD63 #PA5-92370), and Immuno Diagnostics (adiponectin #12010). Blots were visualized using enhanced chemiluminescence (ECL) (Bio-Rad, #1705061) and exposed to X-ray films for development, or by ChemiDoc Imaging System (Bio-Rad) and analyzed by ImageJ.

EV treatment and simulated ischemia or ischemia/reperfusion in cultured cells

In H-only model, EV (10 μg/mL) in 0.5% FBS EV-depleted DMEM was treated right before normoxia or H for 24h using a humidified gas chamber in the CellInsight CX7 High-Content Screening Platform (Thermo Fisher, #HCSDCX7LEDPRO) equilibrated with 1% O2 and 5% CO2 at 37°C. In H/R model, cells were pretreated with EV (10 μg/mL) for 1

hr in 0.5% FBS EV-depleted DMEM, then subjected to H for 24 h and reoxygenation was performed in a standard incubator.

EV characterization analysis

The concentration and size of EV were examined using nanoparticle tracking analysis (NTA). NanoSight (Nanosight Ltd.) with NTA software version 3.4.4 was used. EV samples were diluted in 0.2 μm filtered PBS to concentrations within the machine's optimal detection level. 3 replicates were done for each sample. The temperature was kept between 21.1 to 21.3°C. EV concentrations and size distributions were measured in number of particles per ml and nanometers.

Autophagy HiBiT-LC3 reporter assay

A stable HiBiT-LC3-expressing H9c2 cell line was generated as previously described[99] to study autophagic flux in live cells. Briefly, H9c2 cells were transfected with the autophagy LC3 HiBiT reporter vector (Promega, GA2440) following the manufacturer's instructions [100].

LC3 fused with HaloTag® can react to HaloTag® Ligand and emit fluorescent signals. To validate the responsiveness of the reporter system, cells were treated with 100 nM rapamycin to induce autophagy (Sigma, #RA8781) and 50 nM chloroquine (Sigma, #C6628) to inhibit lysosomal degradation.

After treatment, cells were incubated with Janelia Fluor® 549 HaloTag® Ligand (Promega #GA1110) and nuclear stain for 30 minutes at 37°C to visualize reporter localization in red fluorescent signals captured by Nikon Eclipse Ti2 microscope. Upon autophagy induction, the LC3 reporter is recruited to phagophores and incorporated into autophagosomes, where it is ultimately degraded following lysosomal fusion. Thus, changes in reporter signal reflect dynamic autophagic flux: enhanced autophagy leads to reduced fluorescence due to reporter degradation, while inhibition of autophagy results in signal accumulation.

Oxidative stress assay

ROS production was determined using CellROX™ Red Reagent (Invitrogen, #C10422), which fluoresces upon oxidation (excitation/emission: ~644/665 nm). Cells were stained with 5 μM reagent and nuclear stain in DMEM for 30 min at 37°C, washed with warm PBS, and imaged using the EVOS™ FL Auto 2 Imaging System under 20X (Invitrogen, #AMAFD2000).

Activated caspase 3/7 detection assay

Apoptotic cells were detected using CellEvent™ Caspase-3/7 Green Detection Reagent (Invitrogen, #C10423), which fluoresces as green upon caspase activation. Cells were stained with 2 μM reagent in phenol red-free DMEM, washed with warm PBS, and incubated with nuclear stain for 30 min at 37°C. Fluorescent signals were captured using a Nikon Eclipse Ti2 microscope.

Cell viability assay

Cell viability was analyzed using the ReadyProbes™ Cell Viability Imaging Kit, Blue/Red (Invitrogen, #R37609). Blue dye stains all the nuclei in both live and dead cells, while red dye can only enter and stain nuclei from dead cells. Following media removal and PBS wash, cells were stained with 2 drops/mL of blue/red reagent in phenol red-free DMEM (Gibco™, #11054-020) and incubated for 30 min at 37°C. Fluorescently stained nuclei were imaged using the EVOS™ FL Auto 2 Imaging System, with automated imaging capturing 20% of the same center area of each well under 10X.

Statistics

Data were analyzed using GraphPad Prism 9. Statistical comparisons were performed using an unpaired Student's t-test for two-group comparisons or one-way ANOVA followed by Tukey's multiple comparisons test for comparisons among multiple groups. Data are presented as mean ± SEM, and statistical significance was defined as $P < 0.05$. Outliers were identified and removed using Grubbs' test.

2.4 Results

3-day ALY treatment altered both Ad-EV and plasma-EV characteristics

By tracking particles' Brownian motion under a microscope and applying the Stokes–Einstein equation, NTA was used to assess plasma-EV size and concentration. NTA results (Fig. 5A) showed similar peak sizes (~100 nm) between PBS- and ALY-treated groups. A significant 1.5-fold increase in total ALY-plasma-EV concentration was observed compared to the PBS group (Fig. 5B). ALY-plasma-EV also showed a significant increase in particle concentration within the 90–180 nm size range (Fig. 5C). No significant difference was found in protein amount per EV between PBS and ALY-plasma-EV groups (Fig. 5D).

WB confirmed the phenotype of plasma-EV for EV-associated markers Alix and CD63 (Fig. 5E). Ad-EV were also analyzed; however, CD63 was not tested due to sample limitations (Fig. 5F). Protein concentrations were normalized before analysis, and the presence of adiponectin was confirmed in all EV.

ALY-induced EV activated autophagy, and reduced caspase3/7 activation and cell death upon chronic H

To validate HiBit-LC3 reporter H9c2 reflects autophagic flux, chloroquine and rapamycin were used to inhibit and induce autophagy, respectively (Fig. 6A). Upon inhibition of fusion with lysosomes, autophagosomes consisting of HiBit-Lc3 accumulated and reflected by a stronger fluorescent signal, while rapamycin activated autophagy and the formation of autolysosomes, the fluorescent signal was weaker than the control. ALY-Ad-

EV and ALY-plasma-EV significantly increased autophagic flux compared to the control, while PBS-Ad-EV and PBS-plasma-EV did not change significantly compared to the control (Fig. 6B&C).

Next, caspase 3/7 activation and cell death were examined in H9c2 following 24 h of H. Caspase 3/7 activation showed an apparent increase, and cell death was significantly elevated compared to the control. Both ALY-Ad-EV and ALY-plasma-EV significantly reduced caspase 3/7 activation and cell death compared to H (Fig. 6E & F).

ALY-Ad-EV reduced oxidative stress, caspase 3/7 activation and cell death upon H/R

As ROS generation is an early event in reoxygenation, CellROX staining was performed at 6 hr of H followed by 2 hr of reoxygenation (H/R 6/2 h) to examine oxidative stress (Fig. 7A&B). ROS levels were significantly elevated in the H/R group compared to the control. Treatment with ALY-Ad-EV or ALY-plasma-EV significantly reduced ROS production under H/R conditions.

Caspase-3/7 activation, a hallmark of apoptosis, was investigated at H/R 6/20 hr (Fig. 7C&D). Caspase-3/7 activation was significantly elevated in the H/R group compared to the control. ALY-Ad-EV treatment significantly reduced caspase-3/7 activation, whereas ALY plasma-EV exhibited an apparent but non-significant decrease.

Cell viability was tested using the ReadyProbe cell viability assay 4 h after caspase-3/7 activation (H/R 6/24 h) (Fig. 7E &F). The percentage of cell death was significantly increased in the H/R group compared to controls. ALY-Ad-EV treatment significantly

reduced H/R-induced cell death, whereas ALY plasma-EV exhibited an apparent but non-significant decrease.

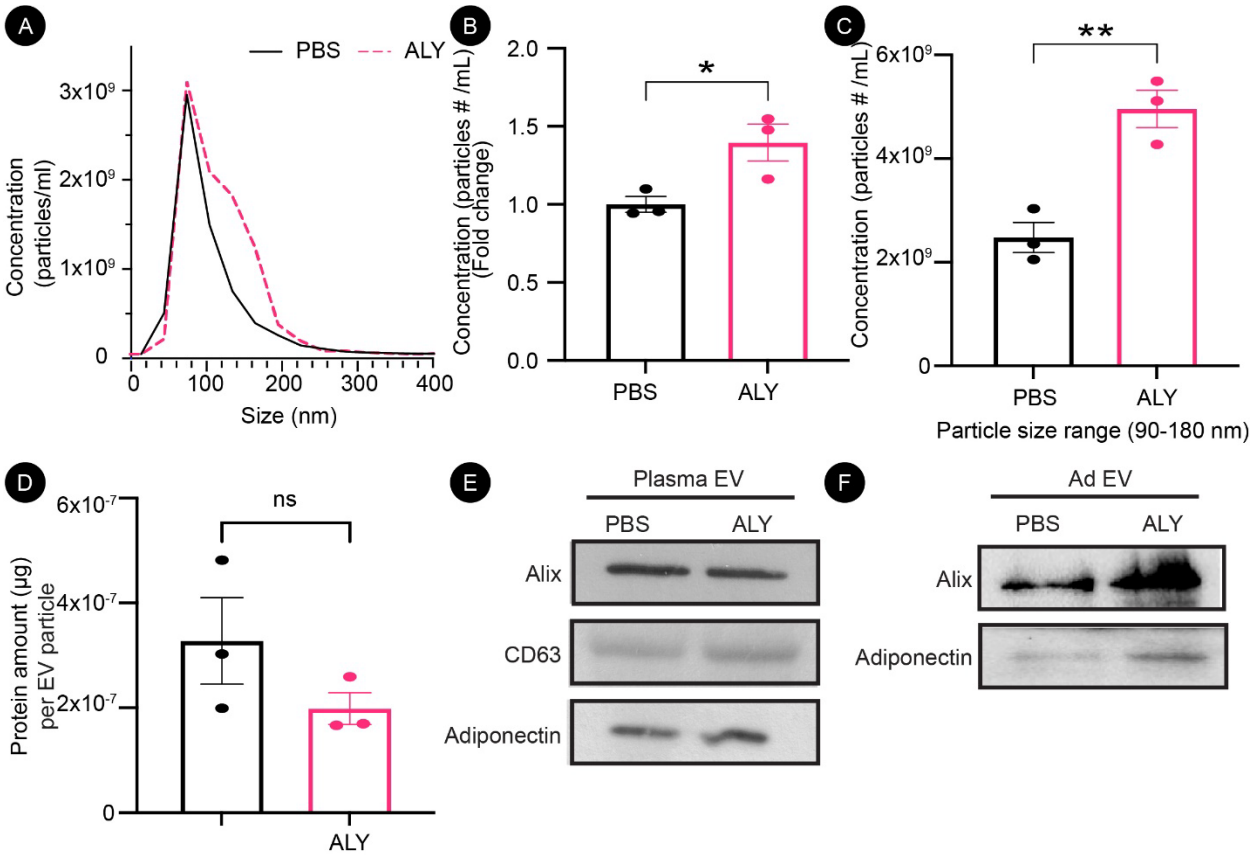

Figure 5. Characterization of plasma- and adipocyte-derived extracellular vesicles (EV) A. The size distribution of plasma PBS/ALY-EV was analyzed by nanoparticle tracking analysis (NTA). (n=3) **B.** Comparison of the total number of plasma PBS/ALY-EV. (n=3) **C.** Comparison of the concentration of plasma PBS/ALY-EV with a size range from 90-180nm. (n=3). **D.** Total protein content per EV particle from plasma PBS/ALY-EV. (n=3) **E.** Representative images of the EV-specific marker Alix & CD63 and adiponectin in plasma-EV from PBS or ALY groups analyzed by western blot (WB). (n=3) **F.** The EV-specific marker Alix, and adiponectin adipocyte-EV from PBS or ALY groups were analyzed by WB. (n=1) T-test and two-way ANOVA were used for the analyses and presented as mean ±SEM. *P<0.05,**<P<0.01, as a significant difference.

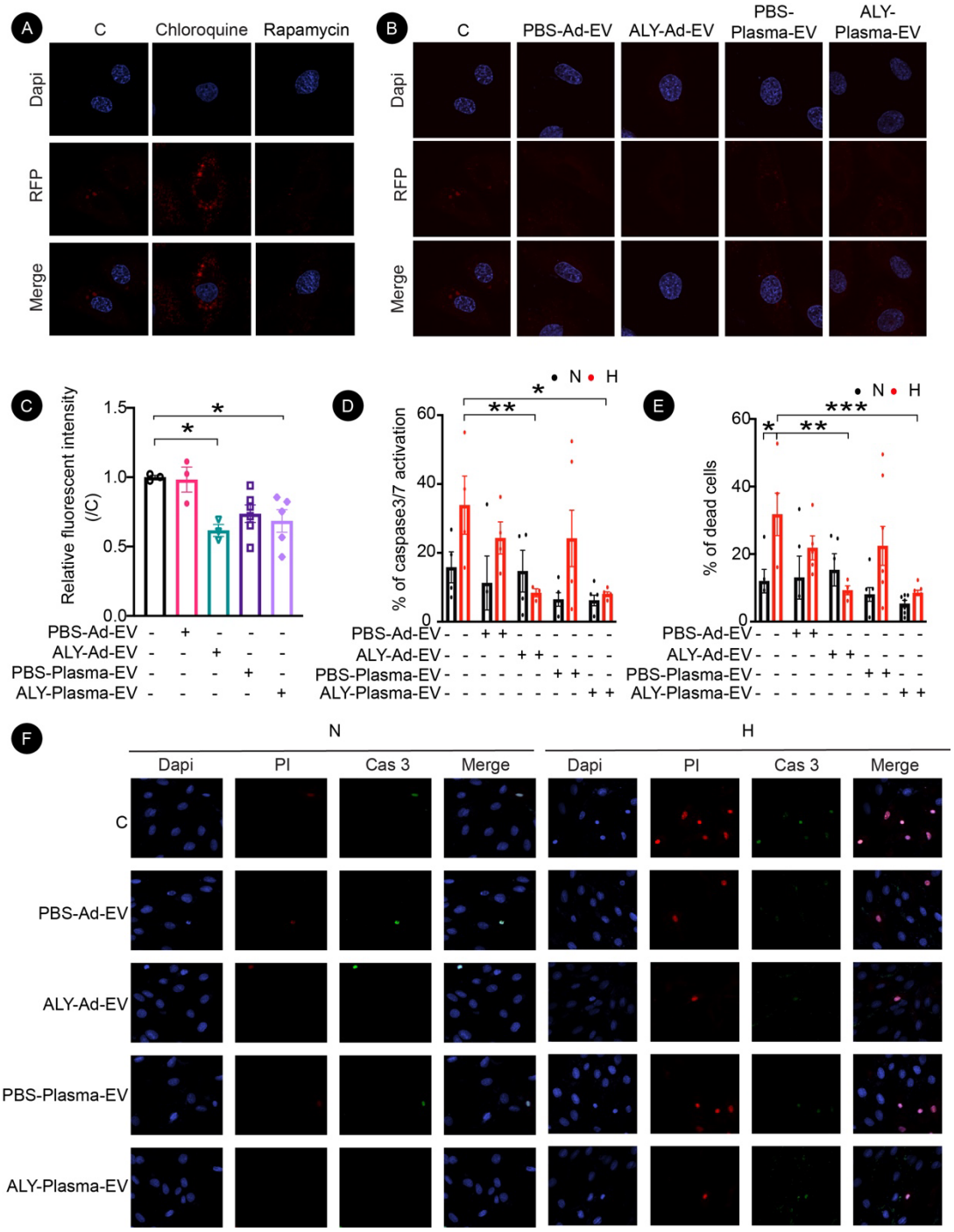

Figure 6. Functional analysis of plasma and adipocyte-derived extracellular vesicles upon 24 hypoxia. A. Representative fluorescence images of functional validation of HiBit-LC3 reporter rat cardiomyoblasts H9c2. **B.** Representative fluorescence images of HiBit-LC3 reporter H9c2 after 1h of EV treatment. **C.** Relative fluorescent intensity was calculated compared to the control. (n=3-6) **D.** The percentage of caspase3/7 activation was calculated and compared between different groups. (n=4) **E**. The percentage of dead cells was calculated and compared between different groups. (n=5-8) **F.** Representative fluorescence images of caspase 3/7 activation (green) and dead cells (red PI staining). One-way ANOVA was used for the analysis and presented as mean ±SEM. *P<0.05,**<P<0.01, ****P<0.0001 as a significant difference.

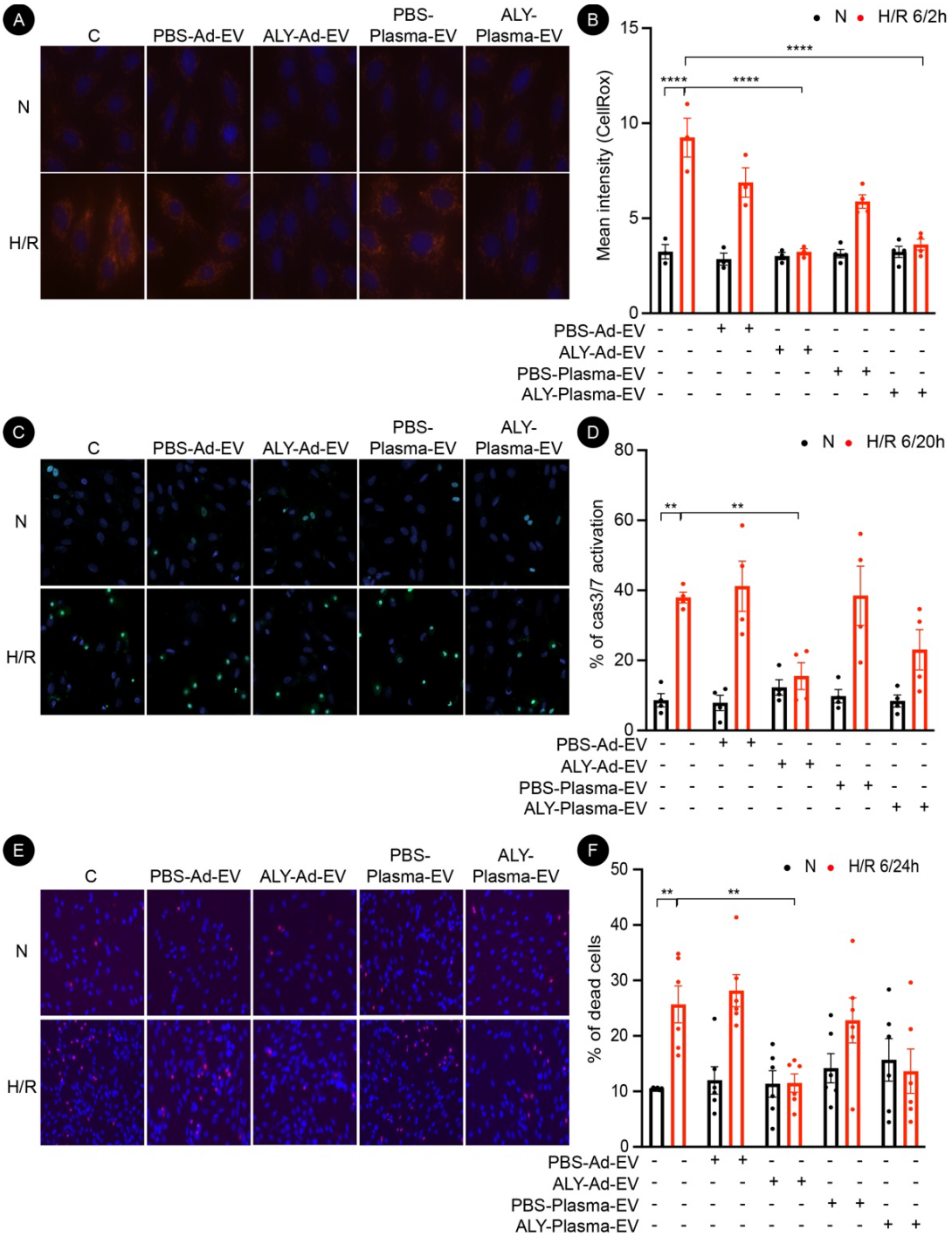

Figure 7. Functional analysis of plasma and adipocyte-derived extracellular vesicles upon hypoxia/reoxygenation(H/R). A. Representative fluorescence images of rat cardiomyoblasts H9c2 stained by CellRox captured after 6 hr H followed by 2 hr R. **B.** Mean intensity per cell was used to compare the level of oxidative stress. (n=4) **C.** Representative fluorescence images of H9c2 stained by Caspase 3/7 reagent captured after 6 hr H followed by 20 hr reoxygenation. **D.** The percentage of caspase3/7 activation was calculated and compared between different groups. (n=4) **E.** Representative fluorescence images of H9c2 stained by ReadyProbe blue/red cell viability reagent captured after 6 hr H followed by 24 hr reoxygenation. **F.** The percentage of dead cells was calculated and compared between different groups. (n=6) One-way ANOVA was used for the analyses and presented as mean ±SEM. *P<0.05, **<P<0.01, ****P<0.0001 as a significant difference.

2.5 Discussion

It has been 30 years since the discovery of adiponectin [1], yet it has not been translated into clinical application. Anti-diabetic drugs such as thiazolidinediones (TZDs) and metformin can increase adiponectin expression by activating PPARα and AMPK [101]; however, this effect depends on the functional status of adipocytes, which may be impaired in cardiometabolic patients. Since the early 2000s, research on EV have expanded rapidly, providing valuable insights into disease mechanisms and therapeutic strategies across a wide range of conditions, including cardiometabolic disorders, cancer, neurodegeneration, and immune regulation [102].

In this study, Ad-EV and plasma-EV were isolated from mice injected with the adiponectin receptor agonist ALY688 and used to evaluate their therapeutic potential against H or H/R injury in H9c2 cells. EV characterization showed notable differences in plasma-EV following ALY688 treatment. Both ALY-Ad-EV and ALY-plasma-EV promoted autophagy under normoxia, and they were able to reduce caspase-3 activation and increase cell viability under H conditions, while also lowering ROS production following H/R. However, under H/R conditions, only ALY-Ad-EV significantly reduced caspase-3 activation and cell death, suggesting a differential potency between EV sources, with ALY-Ad-EV exerting more robust cytoprotective effects under reoxygenation injury.

Several factors may underlie this discrepancy. First, although plasma-EV likely contain a fraction of Ad-EV, the relative abundance is diluted compared to pure Ad-EV. Since equal EV protein concentrations were used for in vitro treatment, the functional dose of Ad-EV

within plasma-EV may be insufficient to replicate the effects seen with isolated Ad-EV. It is well-established that EV therapeutic efficacy follows a dose–response relationship, and both underdosing and overdosing can yield suboptimal outcomes or off-target effects [103]. In vivo, continuous EV release and circulation may compensate for this dilution, but in vitro conditions lack this dynamic replenishment.

This study employed a well-controlled in vitro model that differentiates between H and H/R, enabling precise evaluation of EV-mediated cardioprotection. The comparative analysis of ALY-Ad-EV and ALY-plasma EV, supported by multiple functional assays, offers mechanistic insight into their distinct effects under stress conditions. However, as Ad-EV were isolated ex vivo, their tested properties and functions may not fully reflect in vivo dynamics. The amount of Ad-EV isolated was not enough for NTA analysis; therefore, the size and concentration of EV particles were not characterized. WB EV characterization was not completed either. Additionally, direct evidence of Ad-EV trafficking from adipose tissue to the injured heart has yet to be established to validate the crosstalk effect. Finally, this study focused on adipocytes, but EV derived from other adiponectin-responsive tissues, such as skeletal muscles, liver, and pancreas, were not examined. It remains possible that adiponectin also modulates other cell types that contribute to its overall cardioprotective effects.

Future studies should investigate the biodistribution of ALY-Ad-EV following in vivo administration to determine their circulation patterns and target tissues. The identification of mature adipocyte-specific surface markers would enable in vivo tracking of

endogenous Ad-EV and help to determine whether ALY688 treatment stimulates their production and mobilization to the heart. In parallel, omics-based analyses, such as proteomics and small RNA sequencing, could reveal how ALY688 alters the molecular cargo of both Ad-EV and plasma-EV, potentially uncovering key cardioprotective factors beyond adiponectin, as well as providing deeper insights into adiponectin-related cellular and molecular mechanisms.

Overall, these findings suggest that while both ALY688-induced EV populations confer some degree of protection, ALY-Ad-EV exhibit superior efficacy, particularly under severe stress conditions such as H/R injury. Given that ALY688 activates adiponectin receptor signaling, the enhanced protective effect of ALY-Ad-EV likely reflects their enrichment in adiponectin or adiponectin-responsive cargo. This aligns with previous reports identifying adiponectin as a key mediator of cardioprotection through anti-apoptotic, antioxidant, and autophagy-inducing mechanisms. The data therefore underscore the therapeutic relevance of selectively targeting adipocyte-derived EV as functional carriers of adiponectin-related signals. Furthermore, these findings highlight the importance of optimizing EV therapy not only by source, but also by considering EV dosage, bioactive content, and timing of administration to maximize cardioprotective outcomes.

3 Chapter 3-Therapeutic Potential of Adiponectin-Enriched EV

3.1 Abstract

To overcome the limitations of adiponectin-based therapy, this study developed EV enriched with adiponectin via adiponectin overexpression in human embryonic kidney (HEK) cells and also Wharton's jelly mesenchymal stem cells (WJMSCs). Adiponectin-overexpressing EV (Ad-OE-EV) were characterized and then their functional metabolic effects tested on L6 cells. Both HEK and WJMSCs-derived Ad-OE-EV significantly enhanced insulin-induced Akt phosphorylation, and also caused an apparent increase in glucose uptake. These results highlight the potential of bioengineered EV with high adiponectin content as a promising new approach for metabolic disease intervention.

3.2 Introduction

Adiponectin functions through both endocrine and paracrine pathways to support metabolic homeostasis by regulating glucose and ceramide levels, promoting fatty acid oxidation, and enhancing insulin sensitivity [104]. These effects are mediated through its receptors, AdipoR1 and AdipoR2, which activate pathways such as AMPK and PPARα, promoting glucose uptake and improving mitochondrial function in insulin-responsive tissues [105]. Some common metabolic conditions, including obesity, insulin resistance, and chronic inflammation, are associated with reduced circulating adiponectin [21].

Although adiponectin is a promising therapeutic target, its clinical application remains limited by challenges in producing stable, bioactive recombinant forms. Large-scale production of adiponectin using animal systems also raises concerns related to ethics, immunogenicity, and potential contamination [39]. Protein-based therapies often face the drawback of provoking immune reactions, especially in generating anti-drug antibodies that reduce or block the drug's activity [106]. While adiponectin receptor agonists have demonstrated metabolic benefits in preclinical models, their systemic effects and long-term safety profiles remain unclear.

The therapeutic potential of MSCs is evident in the increasing number of clinical trials exploring their use in treating conditions such as cardiovascular disease, graft-versus-host disease, Crohn's disease, and acute kidney injury [102]. Subsequent findings revealed that the rapid therapeutic effects of MSCs are largely attributed to paracrine mechanisms, particularly the secretion of EV, offering a safer and more scalable

alternative to cell transplantation with reduced risks such as aberrant differentiation or vascular obstruction [102]. MSCs EV carry characteristic surface markers and exert diverse biological effects, including promoting hematopoietic stem cell proliferation and survival, inhibiting B-cell proliferation, and suppressing natural killer cells activity, thereby contributing to immune modulation, tissue repair, and intercellular communication across various physiological and pathological contexts [56]. Among MSC sources, Wharton's Jelly-derived MSCs (from umbilical cord) are particularly attractive due to their accessibility, WJMSCs that can be obtained from the umbilical cord, a medical waste. They have been shown to modulate immune cell activity, inhibit pro-inflammatory cytokine production, and facilitate wound healing and neuroprotection [107].

HEK cells are also one of the cell sources for the scalable production and engineering of EV. Their human origin, high transfection efficiency, and adaptability to serum-free suspension cultures make them ideal for large-scale manufacturing in bioreactors [108]. Importantly, HEK cells are the only immortalized human cell line that has been extensively studied and are not derived from a cancerous origin [109]. Owing to these advantages, HEK cells are frequently used for engineering and modifying EV production [110]. In addition, HEK-derived EVs can enhance the delivery of gene therapies, including adeno-associated viruses, by facilitating targeted transport across tissue barriers [111].

In summary, both WJMSCs-EV and HEK EV are emerging as promising carriers, WJMSCs-EV offer intrinsic therapeutic effects and an established record in regenerative

models, while HEK EV offer a robust, scalable source that can be engineered and produced to clinical-grade standards.

In this study, WJMSCs were transfected with lentivirus overexpressing human adiponectin, and Ad-OE-EV were then collected. As this study was conducted in Dr. Cho's lab in South Korea for a short period, the data are limited. Consequently, I was unable to repeat the study with WJMSCs in our lab here due to various factors, including resource constraints, technical limitations, and regulatory requirements. I then obtained the mouse adiponectin-overexpressing HEK stable cell line from Dr. Xu and extended this project by collecting Ad-OE-EV from HEK. I hypothesize that Ad-OE-EV from both WJMSCs and HEK are enriched with functional adiponectin and will improve insulin responsiveness in L6 cells, supporting their potential as a cell-free therapeutic strategy for metabolic disease intervention.

3.3 Materials and Methods

In vitro cell cultures

Wharton's jelly MSCs (WJMSCs) isolated from human umbilical cord were prepared by Dr. Ssang-Goo Cho's lab in Konkuk University, South Korea. The preparation, isolation and characterization of WJMSCs were previously described [112, 113]. WJMSCs were cultured in complete medium consisting of 10% fetal bovine serum (FBS) (Gibco, #12483-020) and 1% PenStrep (Gibco, #15140) in α-MEM (Gibco, #12571).

Wild-type L6 (ATCC, CRL-1458^{TM}) rat skeletal muscle cells and L6 Akt biosensor cells were used to examine insulin sensitivity. L6 Akt biosensor cells were generated as previously described [45]. Cells were cultured in complete medium consisting of 10% FBS (WISENT, #080-150) and 1% antibiotic-antimycotic (Anti-Anti) (Gibco, #15240) in Alpha Modification of Eagle's Medium (AMEM) (Wisent, #310-010-CL).

Wild-type HEK 293 cells (kindly provided by Dr. Ali Abdul-Sater, York University, Canada) and flag-tagged mouse adiponectin overexpressing HEK 293 cells (kindly provided by Dr. Aimin Xu, Hong Kong University, Hong Kong). Cells were cultured in complete medium consisting of 10% FBS (WISENT, #080-150) and 1% PenStrep (Gibco, #15140) in 4.5 g/L D-glucose DMEM (Gibco, #11965). Unless otherwise specified, all cell cultures were maintained at 37°C in a humidified incubator with 5% CO_2 and subcultured upon reaching ~80% confluency.

Cloning of human adiponectin into lentiviral vector

A mammalian expression plasmid encoding full-length human adiponectin with a C-terminal Flag tag (pCDNA3.1+) stored in filter paper was kindly provided by Dr. Aimin Xu. The plasmid was reconstituted in TE-EF buffer and transformed into competent E. coli and plated on Luria-Bertani (LB) agar with ampicillin. Positive colonies were cultured in LB-ampicillin broth and plasmid DNA was extracted using the NucleoSpin Miniprep Kit. For large-scale preparation, selected clones were expanded in 250 mL LB broth and processed using standard midiprep protocols.

The adiponectin gene was subcloned into a lentiviral backbone vector (pLV-cMVP-MCS-IRES-puro, provided in Dr. Ssang-goo Cho's lab) by restriction digestion and blunt-end ligation. The backbone was digested with MluI (Thermo, #MluI) and BamHI (Thermo, #ER0051), followed by T4 DNA polymerase and dNTPs (NEB). The adiponectin insert was obtained from the mammalian plasmid using BamHI and EcoRV (Thermo, #ER0301) digestion. DNA fragments were extracted from a 1.2% agarose gel using the Cosmo Gel Extraction Kit (Cosmo Bio, #FG-91201). Ligation was performed using T4 DNA ligase (NEB, #M0202) and incubated overnight at 4°C. DNA concentrations were measured using a Nanodrop spectrophotometer, and the ligated product was used for lentivirus production.

Adiponectin-overexpressing lentivirus production in HEK 293T cells

HEK 293T cells were transfected with the adiponectin lentiviral plasmid, the packaging plasmid pAv2, and the envelope plasmid VSV-G using PolyJet transfection reagent,

following the manufacturer's instructions to ensure high transfection efficiency. Conditioned medium containing lentiviral particles was collected over three days. Medium was centrifuged at 4000 rpm for 5 min to remove debris, then filtered through a 0.45 μm syringe filter. The clarified supernatant was transferred to ultracentrifuge tubes and centrifuged at 25,000 rpm for 1.5 h at 4°C. The supernatant was discarded, and the viral pellet was resuspended in 300 μL DMEM-high glucose (Gibco, #11965) by incubation on ice for 1–2 h. The final virus preparation was stored at –80°C until use.

Lentiviral Infection of WJMSCs

WJMSCs were seeded at 1 × 10^6 cells per 10 cm cell culture dish. Lentiviral particles were added to the culture medium along with polybrene (final concentration: 8 μg/mL; Sigma, #TR-1003-G). Cells were divided into three groups: control (polybrene only), empty vector (lentivirus lacking adiponectin), and adiponectin-overexpressing (adiponectin-expressing lentivirus). Infection was performed for no longer than 24 h. After infection, cells were washed with PBS, and the medium was replaced. Once cells reached ~80% confluency, they were switched to EV-depleted medium for EV collection.

Isolation of EV from conditioned media

Cells were cultured in their respective media supplemented with 10% EV-depleted FBS once they reached 70–80% confluency. Conditioned medium was collected daily over 2–3 days, with fresh medium added after each collection. The collected medium was filtered using a 0.2 μm syringe filter (Basix, #13100106), followed by ultracentrifugation at

100,000 × g for 2 hours at 4°C. The supernatant was discarded, and the EV pellet was resuspended in filtered PBS.

Western blot

RIPA buffer (LPS solution, #CBR002) with Halt Protease Inhibitor Cocktails (Thermo, #PI87786) was used for study of WJMSCs. Others were the same as described in Chapter 2. List of antibodies used: Abcam (CD9 #ab263023), Cell Signalling (Alix #92880, anti-rabbit IgG #7074, Calnexin #2433, beta-actin #4970, anti-mouse IgG #7076), Invitrogen (CD63 #PA5-92370), and Immuno Diagnostics (adiponectin #12010).

EV characterization analysis

Same as described in Chapter 2.

Akt signaling dynamics in individual L6 Akt biosensor cells

L6 Akt biosensor cells expressing FoxO1-GFP were used to monitor Akt-mediated translocation of FoxO1 from the nucleus to the cytoplasm in response to insulin. Cells were seeded in 96-well plates at 60–70% confluency, pretreated with EV (10 μg/mL) in AMEM containing 0.5% EV-depleted FBS for 24 h, starved in serum- and EV-free AMEM for 1.5 h, and stimulated with insulin (Lilly, #HI0210) for 10 min. Imaging was performed using the EVOS™ FL Auto 2 Imaging System, capturing 5% of the central area of each well at 20X magnification.

Glucose Uptake Assay

L6 skeletal muscle cells stably overexpressing GLUT4 with an extracellular myc epitope tag were used for glucose uptake analysis. This cell line was originally developed by Dr. Amira Klip (The Hospital for Sick Children, Toronto, Canada) and kindly provided for this study. The assay protocol was adapted from previously published methods[114]. Cells were seeded in 96-well plates and pretreated with EV for 24 h. Following pretreatment, insulin was added at a final concentration of 10 nM for 15 minutes to stimulate glucose uptake. Subsequently, 2-deoxyglucose (2DG) was added and incubated for 30 minutes. The reaction was stopped using the stop buffer provided in the Glucose Uptake-Glo Assay kit (Promega, Cat # J1341), followed by the addition of neutralization buffer. The 2-deoxyglucose-6-phosphate (2DG6P) detection reagent was then applied, and luminescence was measured using a VarioSkan LUX plate reader with an integration time of 0.3 to 1 second.

Phospho-Akt detection in L6 cells

WT L6 cells were seeded in 6-well plates and starved in FBS-free AMEM for 2 h at ~80% confluency, followed by EV treatment (10 µg/mL) for 1 h and insulin stimulation (10 nM) for 10 min. Whole-cell protein lysates and WB analysis were prepared as described above.

Adiponectin measurement by ELISA

Human and mouse adiponectin levels were measured using commercial ELISA kits (IMD, #32010), following the manufacturer's instructions. An equal number of EV particles (1 × 10^9) was used per group for all measurements.

3.4 Results

WJMSCs Ad-OE-EV improve insulin sensitivity in L6 cells

To generate adiponectin-overexpressing EV (Ad-OE-EV), WJMSCs were transduced with a lentiviral vector to overexpress human adiponectin. WB confirmed successful overexpression and secretion of adiponectin in both cells and EV (Fig. 8A–B). EV markers Alix and CD9 were enriched in the EV fraction, while the absence of calnexin confirmed minimal cellular contamination. Nanoparticle tracking analysis (NTA) showed similar size distributions across groups, with a notable increase in EV production (normalized to cell number at the time of collection) in the adiponectin-overexpressing group compared to control and vector groups (Fig. 8C). Functional assessment using L6 Akt biosensor cells showed that WJMSCs Ad-OE-EV significantly enhanced insulin-stimulated Akt activation, as evidenced by a marked reduction in the EC_{50} of insulin, indicating improved insulin sensitivity (Fig. 8D–F).

Characterization of HEK Ad-OE-EV

WB analysis confirmed the overexpression of mouse adiponectin in both HEK cells and Ad-OE-EV, along with established EV markers Alix and CD63, and negative marker calnexin (Fig. 9A&B). However, as HEK cells endogenously express human adiponectin

and the construct overexpresses mouse adiponectin, detection by an anti-mouse adiponectin antibody alone may not fully validate the presence of Ad-OE-EV. To overcome this issue, both mouse and human adiponectin levels were quantified by ELISA. Mouse adiponectin was detected in HEK Ad-OE-EV (7.65 ng/mL), but not in WT EV (Fig. 9E), confirming specific overexpression. In contrast, human adiponectin levels remained below the assay's detection threshold in both groups, with no apparent difference between them (Fig. 9F), indicating that mouse adiponectin overexpression did not affect endogenous expression. NTA showed that Ad-OE-EV had a higher concentration compared to WT-OE-EV (Fig. 9C). However, protein quantification showed apparent lower total protein content per 1×10^9 particles in HEK Ad-OE-EV, suggesting altered cargo composition (Fig. 9D).

HEK Ad-OE-EV enhances insulin-induced Akt activation in L6 cells

To examine the effect of HEK Ad-OE-EV on insulin sensitivity, L6 Akt biosensor cells were treated with HEK WT or Ad-OE-EV, followed by insulin stimulation. HEK Ad-OE-EV treatment significantly enhanced insulin-induced Akt activation compared to PBS and HEK WT EV controls, as demonstrated by increased FoxO1-GFP translocation and a reduced EC_{50} for insulin (Fig. 10A–C), indicating improved insulin sensitivity. To validate the L6 Akt biosensor assay, WB analysis of phosphorylated Akt at Ser473 and glucose uptake were performed. Ser473 is a key regulatory site required for full activation of Akt downstream of insulin signaling. Apparent increase in Akt activation and glucose uptake were observed in L6 treated with Ad-OE-EV compared to WT-EV (Fig. 10D-F). While

these results support the biosensor findings, additional biological replicates will be necessary to confirm reproducibility and statistical significance.

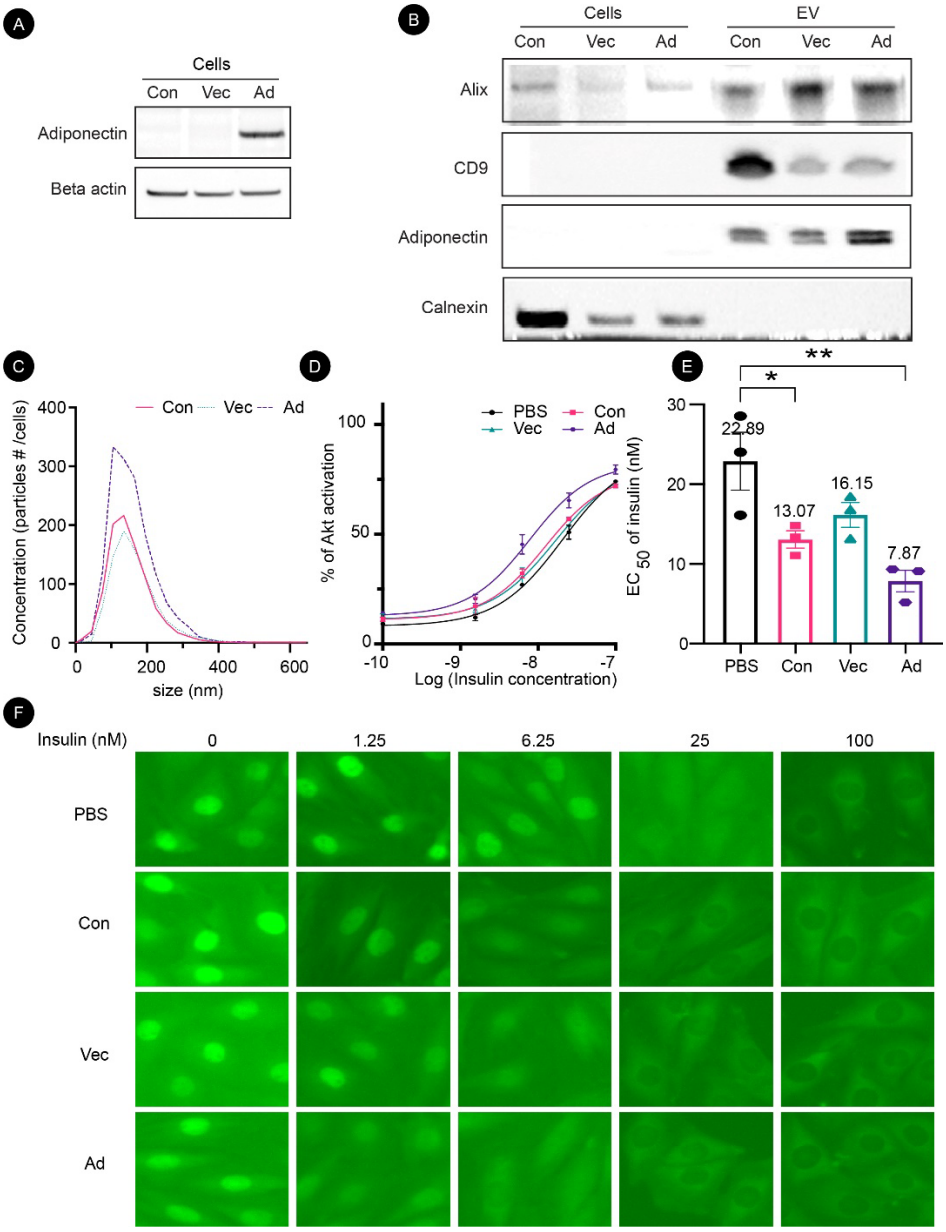

Figure 8. Characterization and functional assessment of adiponectin-overexpressing WJMSC-derived extracellular vesicles (EV). A. Validation of adiponectin overexpression in WJMSCs lysates by western blot (WB). (n=1) **B.** WB of EV markers (Alix, CD9), adiponectin, and negative marker calnexin in cell lysates and EV from control (Con), empty vector (Vec), and adiponectin-overexpressing (Ad) WJMSCs. (n=1) **C.** Size distribution and concentration of EV from each group measured by nanoparticle tracking analysis. (n=1) **D.** Dose–response curves showing Akt activation in L6 Akt biosensor cells treated with WJMSCs EV followed by insulin stimulation. (n=3) **E.** EC_{50} values of insulin for Akt activation calculated from Fig. D. (n=3) **F**. Representative images of FoxO1-GFP translocation in L6 Akt biosensor cells following treatment with PBS, Con EV, Vec EV and Ad-OE-EV and stimulation with increasing concentrations of insulin (0–100 nM). Data are shown as mean ± SEM. (n=3) *p < 0.05, **p < 0.01 by one-way ANOVA with Tukey's multiple comparisons test.

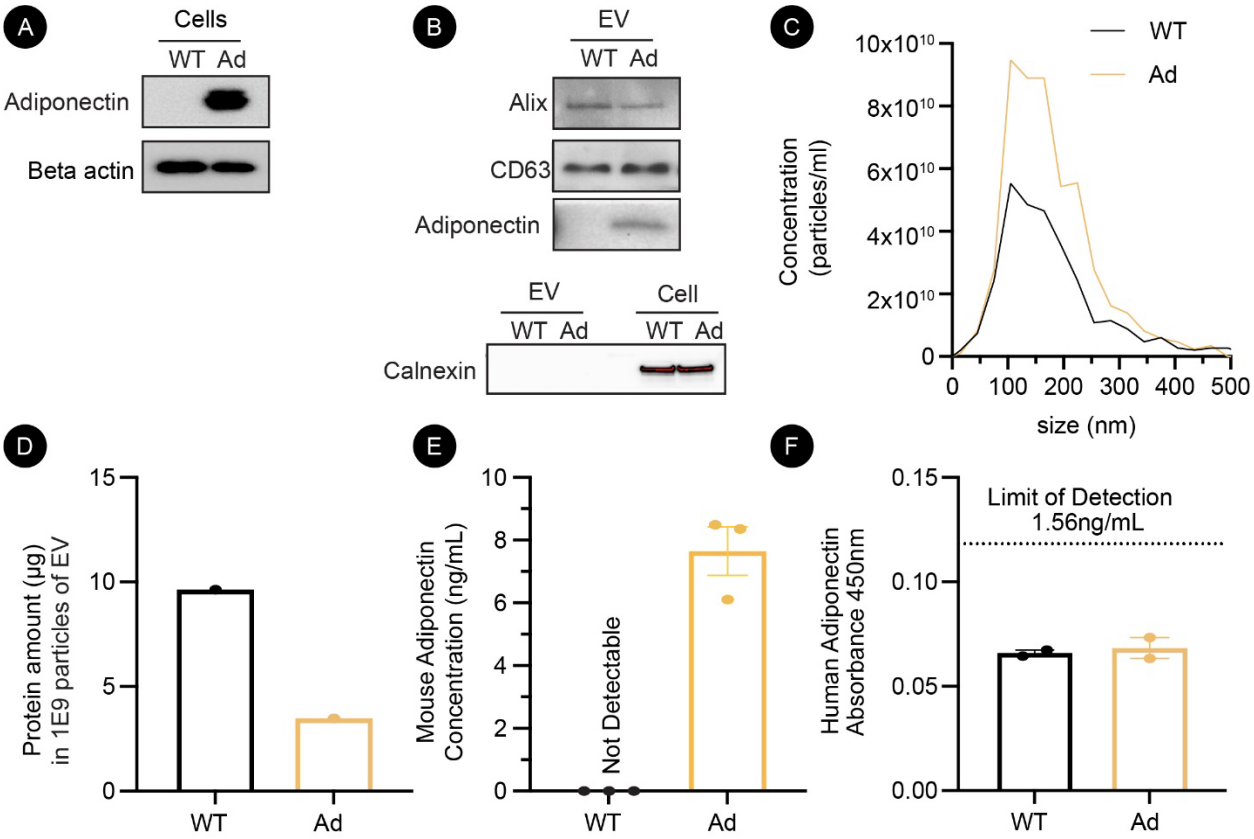

Figure 9. Characterization of EV from wild-type and adiponectin-overexpressing HEK 293 cells. A. Validation of adiponectin overexpression in HEK cells lysates by western blot (WB). (n=1) **B.** WB of EV derived from wild-type (WT) and adiponectin-overexpressing (Ad) HEK cells. Alix and CD63 were used as EV markers. Adiponectin was detected to validate overexpression. The negative marker calnexin was confirmed to be absent from EV. (n=1) **C.** EV size distribution and concentration measured by nanoparticle tracking analysis. (n=1) **D.** Total protein content in 1 × 10^9 EV particles from HEK WT and Ad groups, quantified by BCA assay. (n=1) **E.** Mouse adiponectin levels measured in HEK Ad EV using mouse adiponectin ELISA. (technical n=3) **F.** Human adiponectin levels measured in HEK Ad EV using human adiponectin ELISA. (technical n=2) Data are shown as mean ± SEM.

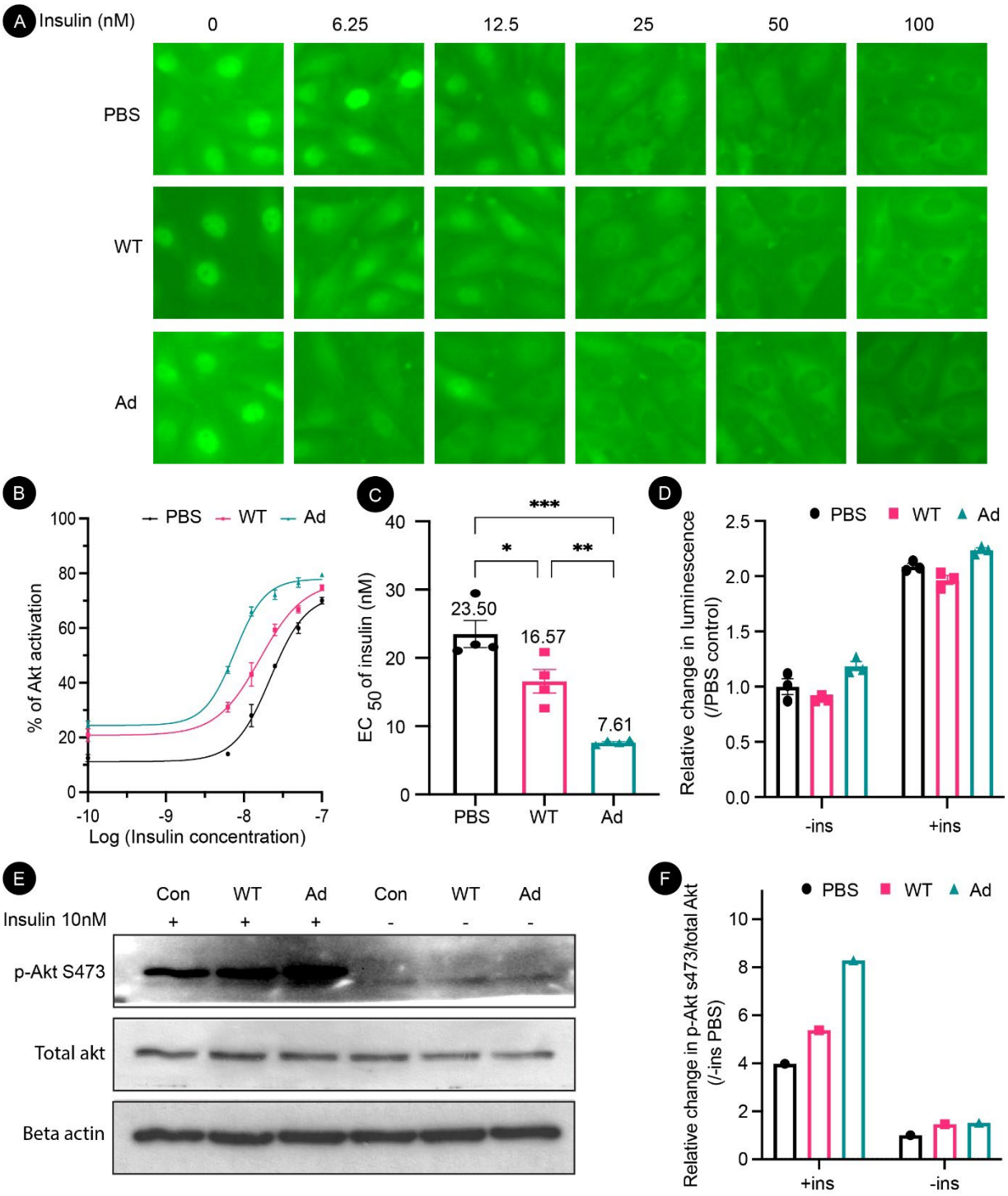

Figure 10. HEK-derived adiponectin-overexpressing extracellular vesicles. A. Representative images of FoxO1-GFP translocation in L6 Akt biosensor cells following treatment with PBS, WT EV, or Ad EV, and stimulation with increasing concentrations of insulin (0–100 nM). **B.** Dose–response curves of Akt activation in L6 cells based on FoxO1-GFP translocation in the nucleus. (n=4) **C.** EC_{50} values of insulin for Akt activation derived from panel B. (n=4) **D.** Effect of EV on glucose uptake in L6 with(+) or without (-) 10nM insulin (ins). (technical n=3) **E&F.** Western blot analysis of p-Akt Ser473 with (+) or without (-) 10 nM insulin treatment followed by EV treatment. (n=1) Data are presented as mean ± SEM. *p < 0.05, **p < 0.01, ***p < 0.001 by one-way ANOVA with Tukey's multiple comparisons test.

3.5 Discussion

Skeletal muscle is responsible for the majority of insulin-stimulated glucose uptake and plays a central role in maintaining systemic glucose homeostasis [115]. Impaired insulin signaling in this tissue is a hallmark of insulin resistance and T2D [116]. Adiponectin is a well-established insulin-sensitizing adipokine [74], which preserves pancreatic β-cell metabolic function by maintaining mitochondrial oxidative phosphorylation and glucose-stimulated insulin secretion [117], and enhances insulin action in skeletal muscle by activating insulin signaling pathways such as AMPK, p-Akt and p-IRS1 [45] in obese or HFD in vivo models.

This study explored the therapeutic potential of engineering Ad-OE-EV as a cell-free strategy to preserve adiponectin bioactivity and enable targeted protein delivery. Adiponectin-overexpressing WJMSCs and HEK cells were utilized for Ad-OE-EV production, revealing two key findings: (1) Ad-OE-EV from both engineered adiponectin-overexpressing WJMSCs and HEK cells contained significantly higher adiponectin levels compared to the control EV, confirming successful enrichment; and (2) control EV from both cell types enhanced insulin sensitivity in L6 cells, while Ad-OE-EV further potentiated this beneficial effect.

MSCs- and HEK-derived EV are both widely utilized for therapeutic delivery of engineered proteins and miRNAs [118]. While MSCs EV often exhibit greater inherent therapeutic potential, MSCs engineering requires more technical complexity and resources. Specifically, establishing stable genetically modified MSCs cell lines is challenging. In this

study, transiently transduced WJMSCs were used for EV isolation, resulting in limited EV yield. Conversely, HEK cells represent a highly established platform with widespread use due to their ease of genetic manipulation, lentiviral transduction efficiency, and stable protein overexpression capabilities. Capitalizing on these advantages, adiponectin-overexpressing stable HEK cell lines were generated to produce higher yields of EV suitable for extensive functional assays.

Consistent with this approach, recent literature demonstrated that WJMSCs engineered to overexpress apelin, an adipokine functionally analogous to adiponectin, successfully reversed insulin resistance and promoted pancreatic β-cell proliferation in T2D rat models [119]. Additionally, high adiponectin expression has been reported to enhance the cardioprotective effects of MSCs by increasing their production of beneficial EV [72], suggesting potential positive feedback mechanisms where adiponectin overexpression may augment therapeutic EV production from MSCs.

This study did not address the metabolic effects or optimal dosage of Ad-OE-EV in vivo, nor did it characterize how the EV cargo profile changes upon adiponectin overexpression. Future studies should address the in vivo therapeutic efficacy of Ad-OE-EV. Given the observed improvements in insulin sensitivity, it is critical to determine the broader effects of Ad-OE-EV on obesity-related metabolic dysfunctions. Comprehensive metabolic profiling following Ad-OE-EV administration to WT and diet-induced obese (DIO) mice, including measurements of insulin sensitivity, fasting blood glucose, glucose tolerance tests (GTT), and metabolic cage analyses (to monitor whole body energy

metabolism), will provide critical insights. Furthermore, evaluating Ad-EV and circulating plasma-EV profiles post-Ad-OE-EV treatment will help elucidate potential systemic impacts and underlying therapeutic mechanisms.

4 Conclusion

This thesis offers new insights into how adiponectin influences EV dynamics to exert cardiac and metabolic benefits. The findings reveal that adiponectin modifies the function of Ad-EV with greater effect than the pool of circulating EV in the plasma in a way that supports cardiomyocyte survival during hypoxia/reoxygenation. In addition, EV enriched with adiponectin improve insulin responsiveness in skeletal muscle cells. These outcomes were demonstrated using both pharmacological stimulation with ALY688 and genetic overexpression strategies. By highlighting EV as downstream effectors of adiponectin signaling, this work adds to the growing body of evidence that EV contribute to inter-organ communication in cardiometabolic regulation. Moreover, the use of engineered EV enriched with adiponectin offers a potential cell-free approach to overcome current limitations in adiponectin-based therapy. Overall, the results emphasize the therapeutic value of targeting EV–adiponectin pathways in the context of cardiometabolic disease.

5 Future directions

This thesis supports the potential role of EV in mediating inter-organ communication and delivering adiponectin in the context of CMD. Future studies should aim to clarify the molecular mechanisms regulating EV biogenesis, cargo selection, and uptake, particularly in tissues and cell types relevant to CMD.

Further methodological development is needed to improve the isolation, characterization, and functional analysis of EV. Standardized approaches will help define EV heterogeneity and examine their distribution and biological activity in relevant disease models.

For therapeutic application, additional efforts are required to optimize EV production, ensure reproducibility, and potentially achieve tissue-specific delivery of bioactive molecules such as adiponectin. Addressing these technical barriers is essential for translating EV-based strategies into clinical use.

Finally, investigation of EV-mediated communication between adipose tissue, skeletal muscle, and the heart may help identify new regulatory pathways and inform the development of EV-based biomarkers and targeted interventions for metabolic and cardiovascular disorders. Incorporating EV analysis into diverse areas of research could offer novel insights and inspire new directions across disciplines.

6 Statement of contributions

Chapter 2

All experiments were designed, conducted, and analyzed by Trista Chung unless otherwise specified. Cindy Sung performed the experiment shown in Fig. 5A. Imaging of the samples I prepared for Fig. 6A–B and 6F was carried out by Jialing Tang.

Chapter 3

All experiments were designed, conducted, and analyzed by Trista Chung unless otherwise specified. Experiments for Fig. 8A–C were performed jointly with Yoojung Kim. Fig. 9B CD63 analysis and Fig. 10D glucose uptake assay were conducted by Khang Nguyen using samples which I prepared. Fig. 9C was performed by Jialing Tang, while Fig. 9E-F were performed by Yubin Lei.

7 References

1. Scherer, P.E., et al., A novel serum protein similar to C1q, produced exclusively in adipocytes. J Biol Chem, 1995. 270(45): p. 26746-9.
2. Wang, Y., et al., Cardiomyocyte-derived adiponectin is biologically active in protecting against myocardial ischemia-reperfusion injury. Am J Physiol Endocrinol Metab, 2010. 298(3): p. E663-70.
3. Jasinski-Bergner, S., et al., Adiponectin and Its Receptors Are Differentially Expressed in Human Tissues and Cell Lines of Distinct Origin. Obes Facts, 2017. 10(6): p. 569-583.
4. Ding, X., et al., The roles of leptin and adiponectin: a novel paradigm in adipocytokine regulation of liver fibrosis and stellate cell biology. American Journal of Pathology, 2005. 166(6).
5. Halberg, N., et al., Systemic fate of the adipocyte-derived factor adiponectin. Diabetes, 2009. 58(9): p. 1961-70.
6. Kubota, N., et al., Adiponectin stimulates AMP-activated protein kinase in the hypothalamus and increases food intake. Cell Metab, 2007. 6(1): p. 55-68.
7. Khoramipour, K., et al., Adiponectin: Structure, Physiological Functions, Role in Diseases, and Effects of Nutrition. Nutrients, 2021. 13(4).
8. Park, H.S., et al., PPARgamma neddylation essential for adipogenesis is a potential target for treating obesity. Cell Death Differ, 2016. 23(8): p. 1296-311.
9. Khan, S. and C.H. Wang, ER stress in adipocytes and insulin resistance: mechanisms and significance (Review). Mol Med Rep, 2014. 10(5): p. 2234-40.
10. Straub, L.G. and P.E. Scherer, Metabolic Messengers: Adiponectin. Nat Metab, 2019. 1(3): p. 334-339.
11. Suzuki, S., et al., The Oligomeric Structure of High Molecular Weight Adiponectin. FEBS Lett., 2007. 581(5).
12. Fruebis, J., et al., Proteolytic cleavage product of 30-kDa adipocyte complement-related protein increases fatty acid oxidation in muscle and causes weight loss in mic. Proc Natl Acad Sci U S A, 2001. 98(4).
13. Fiaschi, T., et al., Globular adiponectin induces differentiation and fusion of skeletal muscle cells. Cell Res, 2009. 19(5): p. 584-97.
14. Vionnet, N., et al., Genomewide search for type 2 diabetes-susceptibility genes in French whites: evidence for a novel susceptibility locus for early-onset diabetes on chromosome 3q27-qter and independent replication of a type 2-diabetes locus on chromosome 1q21-q24. Am J Hum Genet, 2000. 67(6).
15. Francke, S., et al., A genome-wide scan for coronary heart disease suggests in Indo-Mauritians a susceptibility locus on chromosome 16p13 and replicates linkage with the metabolic syndrome on 3q27. Human Molecular Genetics, 2001. 10(24).
16. Jeerawattanawart, S., et al., Regulation and function of adiponectin in the intestinal epithelial cells in response to Trichinella spiralis infection. Sci Rep, 2023. 13(1): p. 14004.
17. Li, T.D. and Z.H. Zeng, Adiponectin as a potential therapeutic target for the treatment of restenosis. Biomed Pharmacother, 2018. 101: p. 798-804.

18. Braun, L.M., et al., Adiponectin reduces immune checkpoint inhibitor-induced inflammation without blocking anti-tumor immunity. Cancer Cell, 2025. 43(2): p. 269-291 e19.
19. Yamauchi, T. and T. Kadowaki, Adiponectin receptor as a key player in healthy longevity and obesity-related diseases. Cell Metab, 2013. 17(2): p. 185-96.
20. Zhao, S., C.M. Kusminski, and P.E. Scherer, Adiponectin, Leptin and Cardiovascular Disorders. Circulation Research 2021. 128(1): p. 136-149.
21. Trujillo, M.E. and P.E. Scherer, Adiponectin--journey from an adipocyte secretory protein to biomarker of the metabolic syndrome. J Intern Med, 2005. 257(2): p. 167-75.
22. Yamauchi, T., et al., Cloning of adiponectin receptors that mediate antidiabetic metabolic effects. Nature, 2003. 423(6941): p. 762-9.
23. Yamauchi, T., et al., Targeted disruption of AdipoR1 and AdipoR2 causes abrogation of adiponectin binding and metabolic actions. Nat Med, 2007. 13(3): p. 332-9.
24. Yamauchi, T., et al., Adiponectin stimulates glucose utilization and fatty-acid oxidation by activating AMP-activated protein kinase. Nat Med, 2002. 8(11): p. 1288-95.
25. Iwabu, M., et al., Adiponectin and AdipoR1 regulate PGC-1alpha and mitochondria by Ca(2+) and AMPK/SIRT1. Nature, 2010. 464(7293): p. 1313-9.
26. Yoon, Y.S., et al., Adiponectin and thiazolidinedione targets CRTC2 to regulate hepatic gluconeogenesis. Exp Mol Med, 2009. 41(8): p. 577-83.
27. Yamauchi, T., et al., The fat-derived hormone adiponectin reverses insulin resistance associated with both lipoatrophy and obesity. Nat Med, 2001. 7(8): p. 941-6.
28. Hug, C., et al., T-cadherin is a receptor for hexameric and high-molecular-weight forms of Acrp30/adiponectin. Proc Natl Acad Sci U S A., 2004. 101(28): p. 10308-13.
29. Denzel, M.S., et al., T-cadherin is critical for adiponectin-mediated cardioprotection in mice. J Clin Invest, 2010. 120(12): p. 4342-52.
30. Shibata, R., et al., Adiponectin protects against myocardial ischemia-reperfusion injury through AMPK- and COX-2-dependent mechanisms. Nat Med, 2005. 11(10): p. 1096-103.
31. Antonopoulos, A.S., et al., Mutual Regulation of Epicardial Adipose Tissue and Myocardial Redox State by PPAR-gamma/Adiponectin Signalling. Circ Res, 2016. 118(5): p. 842-55.
32. Scheja, L. and J. Heeren, The endocrine function of adipose tissues in health and cardiometabolic disease. Nat Rev Endocrinol, 2019. 15(9): p. 507-524.
33. Tao, L., et al., Adiponectin cardioprotection after myocardial ischemia/reperfusion involves the reduction of oxidative/nitrative stress. Circulation, 2007. 115(11): p. 1408-16.
34. Hopkins, T.A., et al., Adiponectin actions in the cardiovascular system. Cardiovasc Res., 2007. 74(1): p. 11-8.
35. Kim, J., et al., AMPK and mTOR regulate autophagy through direct phosphorylation of Ulk1. Nat Cell Biol, 2011. 13(2): p. 132-41.

36. Kitada, M. and D. Koya, Autophagy in metabolic disease and ageing. Nat Rev Endocrinol, 2021. 17(11): p. 647-661.
37. Holland, W.L. and S.A. Summers, Strong Heart, Low Ceramides. Diabetes, 2018. 67(8): p. 1457-1460.
38. Holland, W.L., et al., The Pleiotropic Actions of Adiponectin are Initiated via Receptor-Mediated Activation of Ceramidase Activity. Nat Med, 2011. 17(1): p. 55-63.
39. Yoo, E., et al., Sustainable production of multimeric and functional recombinant human adiponectin using genome-edited chickens. J Biol Eng, 2024. 18(1): p. 32.
40. Okada-Iwabu, M., et al., A small-molecule AdipoR agonist for type 2 diabetes and short life in obesity. Nature, 2013. 503(7477): p. 493-9.
41. Otvos, L., Jr., et al., Design and development of a peptide-based adiponectin receptor agonist for cancer treatment. BMC Biotechnol, 2011. 11: p. 90.
42. Otvos, L., Jr., Potential Adiponectin Receptor Response Modifier Therapeutics. Front Endocrinol (Lausanne), 2019. 10: p. 539.
43. Tan, W., et al., AdipoRon ameliorates the progression of heart failure with preserved ejection fraction via mitigating lipid accumulation and fibrosis. J Adv Res, 2025. 68: p. 299-315.
44. Selvais, C.M., et al., AdipoRon enhances healthspan in middle-aged obese mice: striking alleviation of myosteatosis and muscle degenerative markers. J Cachexia Sarcopenia Muscle, 2023. 14(1): p. 464-478.
45. Sung, H.K., et al., ALY688 elicits adiponectin-mimetic signaling and improves insulin action in skeletal muscle cells. Am J Physiol Cell Physiol, 2022. 322(2): p. C151-C163.
46. Cho, S., et al., Cardioprotection by the adiponectin receptor agonist ALY688 in a preclinical mouse model of heart failure with reduced ejection fraction (HFrEF). Biomed Pharmacother, 2024. 171: p. 116119.
47. Liu, Y., V. Vu, and G. Sweeney, Examining the Potential of Developing and Implementing Use of Adiponectin-Targeted Therapeutics for Metabolic and Cardiovascular Diseases. Front Endocrinol (Lausanne), 2019. 10: p. 842.
48. Kalluri, R. and V.S. LeBleu, The biology, function, and biomedical applications of exosomes. Science, 2020. 367(6478).
49. Han, C., et al., Extracellular vesicles in cardiovascular disease: Biological functions and therapeutic implications. Pharmacol Ther, 2022. 233: p. 108025.
50. Akers, J.C., et al., Biogenesis of extracellular vesicles (EV): exosomes, microvesicles, retrovirus-like vesicles, and apoptotic bodies. J Neurooncol, 2013. 113(1): p. 1-11.
51. Welsh, J.A., et al., Minimal information for studies of extracellular vesicles (MISEV2023): From basic to advanced approaches. J Extracell Vesicles, 2024. 13(2): p. e12404.
52. van de Wakker, S.I., et al., Size matters: Functional differences of small extracellular vesicle subpopulations in cardiac repair responses. J Extracell Vesicles, 2024. 13(1): p. e12396.
53. Akbar, N., et al., Extracellular vesicles in metabolic disease. Diabetologia, 2019. 62(12): p. 2179-2187.

54. Crewe, C., et al., Extracellular vesicle-based interorgan transport of mitochondria from energetically stressed adipocytes. Cell Metab, 2021. 33(9): p. 1853-1868 e11.
55. Liu, J., et al., Integrative biology of extracellular vesicles in diabetes mellitus and diabetic complications. Theranostics, 2022. 12(3): p. 1342-1372.
56. Kumar, M.A., et al., Extracellular vesicles as tools and targets in therapy for diseases. Signal Transduct Target Ther, 2024. 9(1): p. 27.
57. Rai, A., et al., The Discovery of Extracellular Vesicles and Their Emergence as a Next-Generation Therapy. Circ Res, 2024. 135(1): p. 198-221.
58. Gross, R., et al., Phosphatidylserine-exposing extracellular vesicles in body fluids are an innate defence against apoptotic mimicry viral pathogens. Nat Microbiol, 2024. 9(4): p. 905-921.
59. O'Reilly, D., et al., Perspective: The Role of Human Breast-Milk Extracellular Vesicles in Child Health and Disease. Adv Nutr, 2021. 12(1): p. 59-70.
60. Ohayon, L., X. Zhang, and P. Dutta, The role of extracellular vesicles in regulating local and systemic inflammation in cardiovascular disease. Pharmacol Res, 2021. 170: p. 105692.
61. Yang, C., et al., Extracellular vesicles and their engineering strategies, delivery systems, and biomedical applications. J Control Release, 2024. 365: p. 1089-1123.
62. Liang, X., et al., Engineering of extracellular vesicles for efficient intracellular delivery of multimodal therapeutics including genome editors. Nat Commun, 2025. 16(1): p. 4028.
63. Kim, H.I., et al., Recent advances in extracellular vesicles for therapeutic cargo delivery. Exp Mol Med, 2024. 56(4): p. 836-849.
64. Wang, X., et al., Engineered Exosomes With Ischemic Myocardium-Targeting Peptide for Targeted Therapy in Myocardial Infarction. J Am Heart Assoc, 2018. 7(15): p. e008737.
65. Zhu, L.P., et al., Hypoxia-elicited mesenchymal stem cell-derived exosomes facilitates cardiac repair through miR-125b-mediated prevention of cell death in myocardial infarction. Theranostics, 2018. 8(22): p. 6163-6177.
66. Belhadj, Z., et al., A combined "eat me/don't eat me" strategy based on extracellular vesicles for anticancer nanomedicine. J Extracell Vesicles, 2020. 9(1): p. 1806444.
67. Lv, K., et al., Incorporation of small extracellular vesicles in sodium alginate hydrogel as a novel therapeutic strategy for myocardial infarction. Theranostics, 2019. 9(24): p. 7403-7416.
68. Nakase, I., et al., Arginine-rich cell-penetrating peptide-modified extracellular vesicles for active macropinocytosis induction and efficient intracellular delivery. Sci Rep, 2017. 7(1): p. 1991.
69. Nakase, I. and S. Futaki, Combined treatment with a pH-sensitive fusogenic peptide and cationic lipids achieves enhanced cytosolic delivery of exosomes. Sci Rep, 2015. 5: p. 10112.
70. Kita, S., N. Maeda, and I. Shimomura, Interorgan communication by exosomes, adipose tissue, and adiponectin in metabolic syndrome. J Clin Invest, 2019. 129(10): p. 4041-4049.

71. Obata, Y., et al., Adiponectin/T-cadherin system enhances exosome biogenesis and decreases cellular ceramides by exosomal release. JCI Insight, 2018. 3(8).
72. Nakamura, Y., et al., Adiponectin Stimulates Exosome Release to Enhance Mesenchymal Stem-Cell-Driven Therapy of Heart Failure in Mice. Mol Ther, 2020. 28(10): p. 2203-2219.
73. Fisman, E.Z. and A. Tenenbaum, Adiponectin: a manifold therapeutic target for metabolic syndrome, diabetes, and coronary disease? Cardiovasc Diabetol, 2014. 13: p. 103.
74. Kadowaki, T., et al., Adiponectin and adiponectin receptors in insulin resistance, diabetes, and the metabolic syndrome. J Clin Invest, 2006. 116(7): p. 1784-92.
75. Deng, Z.B., et al., Adipose tissue exosome-like vesicles mediate activation of macrophage-induced insulin resistance. Diabetes, 2009. 58(11): p. 2498-505.
76. Michel, L.Y.M., Extracellular Vesicles in Adipose Tissue Communication with the Healthy and Pathological Heart. Int J Mol Sci, 2023. 24(9).
77. Fruhbeck, G., et al., Adiponectin-leptin ratio: A promising index to estimate adipose tissue dysfunction. Relation with obesity-associated cardiometabolic risk. Adipocyte, 2018. 7(1): p. 57-62.
78. Nikolajevic, J., et al., The Role of MicroRNAs in Endothelial Cell Senescence. Cells, 2022. 11(7).
79. Sun, T., et al., MicroRNA let-7 regulates 3T3-L1 adipogenesis. Mol Endocrinol, 2009. 23(6): p. 925-31.
80. Lin, Q., et al., A role of miR-27 in the regulation of adipogenesis. FEBS J, 2009. 276(8): p. 2348-58.
81. Fruhbeis, C., D. Frohlich, and E.M. Kramer-Albers, Emerging roles of exosomes in neuron-glia communication. Front Physiol, 2012. 3: p. 119.
82. Thomou, T., et al., Adipose-derived circulating miRNAs regulate gene expression in other tissues. Nature, 2017. 542(7642): p. 450-455.
83. Blandin, A., et al., Extracellular vesicles are carriers of adiponectin with insulin-sensitizing and anti-inflammatory properties. Cell Rep, 2023. 42(8): p. 112866.
84. Fu, Y., et al., Adiponectin promotes adipocyte differentiation, insulin sensitivity, and lipid accumulation. J Lipid Res, 2005. 46(7): p. 1369-79.
85. Heusch, G., Myocardial ischaemia-reperfusion injury and cardioprotection in perspective. Nat Rev Cardiol, 2020. 17(12): p. 773-789.
86. Cadenas, S., ROS and redox signaling in myocardial ischemia-reperfusion injury and cardioprotection. Free Radic Biol Med, 2018. 117: p. 76-89.
87. Dharmakumar, R., et al., Reperfused Myocardial Infarction: The Road to CCS Classification of Acute MI and Beyond. JACC Adv, 2025. 4(2): p. 101528.
88. Sun, Y., et al., Adiponectin exerts cardioprotection against ischemia/reperfusion injury partially via calreticulin mediated anti-apoptotic and anti-oxidative actions. Apoptosis, 2017. 22(1): p. 108-117.
89. Jang, A.Y., et al., Adiponectin and cardiometabolic trait and mortality: where do we go? Cardiovasc Res, 2022. 118(9): p. 2074-2084.
90. Wang, Y., X.L. Ma, and W.B. Lau, Cardiovascular Adiponectin Resistance: The Critical Role of Adiponectin Receptor Modification. Trends Endocrinol Metab, 2017. 28(7): p. 519-530.

91. Zhu, D., et al., Targeting Adiponectin Receptor 1 Phosphorylation Against Ischemic Heart Failure. Circ Res, 2022. 131(2): p. e34-e50.
92. Gan, L., et al., Adipocyte-derived small extracellular vesicles exacerbate diabetic ischemic heart injury by promoting oxidative stress and mitochondrial-mediated cardiomyocyte apoptosis. Redox Biol, 2025. 79: p. 103443.
93. Loyer, X., C.M. Boulanger, and S. Le Lay, Adipocyte extracellular vesicles: rescuers of cardiac mitochondrial stress. Trends Endocrinol Metab, 2022. 33(1): p. 1-3.
94. Dietze-Schroeder, D., et al., Autocrine action of adiponectin on human fat cells prevents the release of insulin resistance-inducing factors. . Diabetes, 2003. 54(7): p. 2003-11.
95. Osuru, H.P., M. Lavallee, and R.H. Thiele, Molecular and Cellular Response of the Myocardium (H9C2 Cells) Towards Hypoxia and HIF-1alpha Inhibition. Front Cardiovasc Med, 2022. 9: p. 711421.
96. Tam, E., et al., Autophagy deficiency exacerbated hypoxia-reoxygenation induced inflammation and cell death via a mitochondrial DNA/STING/IRF3 pathway. Life Sci, 2024. 358: p. 123173.
97. Xiang, M., et al., Role of Oxidative Stress in Reperfusion following Myocardial Ischemia and Its Treatments. Oxid Med Cell Longev, 2021. 2021: p. 6614009.
98. Del Re, D.P., et al., Fundamental Mechanisms of Regulated Cell Death and Implications for Heart Disease. Physiol Rev, 2019. 99(4): p. 1765-1817.
99. Tang, J., et al., Impaired autophagy flux contributes to enhanced ischemia reperfusion injury in the diabetic heart. Autophagy Rep, 2024. 3(1): p. 2330327.
100. Velagapudi, R., et al., Induction of Autophagy and Activation of SIRT-1 Deacetylation Mechanisms Mediate Neuroprotection by the Pomegranate Metabolite Urolithin A in BV2 Microglia and Differentiated 3D Human Neural Progenitor Cells. Mol Nutr Food Res, 2019. 63(10): p. e1801237.
101. Begum, M., et al., Adiponectin: A Promising Target for the Treatment of Diabetes and Its Complications. Life (Basel), 2023. 13(11).
102. EL Andaloussi, S., et al., Extracellular vesicles: biology and emerging therapeutic opportunities. Nat Rev Drug Discov, 2013. 12(5): p. 347-57.
103. Gupta, D., A.M. Zickler, and S. El Andaloussi, Dosing extracellular vesicles. Adv Drug Deliv Rev, 2021. 178: p. 113961.
104. Li, Y., T. Onodera, and P.E. Scherer, Adiponectin. Trends Endocrinol Metab, 2024. 35(7): p. 674-675.
105. Roy, B. and S.S. Palaniyandi, Tissue-specific role and associated downstream signaling pathways of adiponectin. Cell Biosci, 2021. 11(1): p. 77.
106. Carter PJ and Q. V, Immunogenicity risk assessment and mitigation for engineered antibody and protein therapeutics. . Nat Rev Drug Discov., 2024. 23(12): p. 898-913.
107. Joerger-Messerli, M.S., et al., Mesenchymal Stem Cells from Wharton's Jelly and Amniotic Fluid. Best Pract Res Clin Obstet Gynaecol, 2016. 31: p. 30-44.
108. Vo, N., et al., A novel multi-stage enrichment workflow and comprehensive characterization for HEK293F-derived extracellular vesicles. J Extracell Vesicles, 2024. 13(5): p. e12454.

109. Kim, J., et al., Platform technologies and human cell lines for the production of therapeutic exosomes. Extracell Vesicles Circ Nucl Acids, 2021. 2(1): p. 3-17.
110. Wang, C., et al., Engineering a HEK-293T exosome-based delivery platform for efficient tumor-targeting chemotherapy/internal irradiation combination therapy. J Nanobiotechnology, 2022. 20(1): p. 247.
111. Kwak, G., et al., Extracellular vesicles enhance pulmonary transduction of stably associated adeno-associated virus following intratracheal administration. J Extracell Vesicles, 2023. 12(6): p. e12324.
112. Lim, K.M., et al., High Therapeutic and Esthetic Properties of Extracellular Vesicles Produced from the Stem Cells and Their Spheroids Cultured from Ocular Surgery-Derived Waste Orbicularis Oculi Muscle Tissues. Antioxidants (Basel), 2021. 10(8).
113. Kim, K., et al., Improved Isolation and Culture of Urine-Derived Stem Cells (USCs) and Enhanced Production of Immune Cells from the USC-Derived Induced Pluripotent Stem Cells. J Clin Med, 2020. 9(3).
114. Palanivel, R., et al., Adiponectin stimulates Rho-mediated actin cytoskeleton remodeling and glucose uptake via APPL1 in primary cardiomyocytes. Metabolism, 2014. 63(10): p. 1363-73.
115. Richter, E.A., P.J. Bilan, and A. Klip, A comprehensive view of muscle glucose uptake: regulation by insulin, contractile activity, and exercise. Physiol Rev, 2025. 105(3): p. 1867-1945.
116. DeFronzo, R.A. and D. Tripathy, Skeletal muscle insulin resistance is the primary defect in type 2 diabetes. Diabetes Care, 2009. 32 Suppl 2(Suppl 2): p. S157-63.
117. Munhoz, A.C., et al., Adiponectin reverses beta-Cell damage and impaired insulin secretion induced by obesity. Aging Cell, 2023. 22(6): p. e13827.
118. Wiklander, O.P.B., et al., Advances in therapeutic applications of extracellular vesicles. Sci Transl Med, 2019. 11(492).
119. Gao, L.R., et al., Overexpression of apelin in Wharton' jelly mesenchymal stem cell reverses insulin resistance and promotes pancreatic beta cell proliferation in type 2 diabetic rats. Stem Cell Res Ther, 2018. 9(1): p. 339.